associated to either apoptosis or cell cycle pathway. Therefore, we studied the effect of SN-38 either transiently present for 2 hours or after further incubation for 72 hours in the presence and absence of 50 μmol/L UDCA on the mRNA expression level of various proteins associated to these respective pathways. SN-38 reduced the mRNA level of Bcl-x_L, p16, and c-fos by 30% to 50% but did not affect the mRNA expression level of Bax, Bcl-2, p21, and p15. The HT-29 cells have a mutated p53; therefore, this was used as an additional internal control. However, in these experiments, it was clear that UDCA had no significant effect either alone or when added after removal of SN-38 on the mRNA level of these proteins (data not shown). These results on the lack of effect of UDCA on transcriptional regulation of proteins of the cell cycle are supportive of the above report that UDCA did not alter the SN-38-induced cell cycle arrest.

Effect of UDCA on $\Delta\Psi_m$

The involvement of the mitochondria in the apoptotic effect of SN-38 and UDCA was investigated. When the mitochondrial membrane is hyperpolarized, JC-1 forms J-aggregates in the mitochondria, which emit a red orange fluorescence detectable at 490-nm wavelength. However, when the mitochondrial membrane is depolarized, JC-1 emits a green fluorescence detectable at 525 nm. First, we used 1 μmol/L FCCP, a proton ionophore that is well known to depolarize $\Delta\Psi_m$. Five to 10 minutes after application of FCCP, the population of cells detected at 525 nm increased, whereas that at 490 nm decreased, indicating that the mitochondrial membrane was depolarized (data not shown). Next, the effect of 1 μmol/L SN-38 and 100 μmol/L UDCA on the $\Delta\Psi_m$ over a period of 48 hours was investigated. Up to 6 hours, the number of cells with depolarized mitochondria was not altered by either SN-38 or UDCA alone. After 24 hours, this number was not significantly increased by SN-38 alone, whereas SN-38 followed by 24-hour incubation with 100 μmol/L UDCA induced a significant ($P < 0.01$) increase in cells with depolarized mitochondria by ~250% when compared with control (Fig. 5A). By 48 hours, the percentage of cells with depolarized mitochondria was similarly increased by SN-38 alone (~300%) or by SN-38 followed by UDCA for 48 hours (~330%).

This was also confirmed by the visualization of depolarized mitochondria using confocal laser scanning microscopy with TMRM and calcein-AM according to the method developed by Nieminen et al. (22). Figure 5B and C reports a change in shape of the cells following SN-38 treatment for 48 hours. The HT-29 cells were rounder, larger, and positioned at a higher Z-axis from the bottom plane and were termed round cells. This was shown in a reconstructed three-dimensional image (Fig. 5C). This SN-38-induced increase in cell volume was cell density independent (data not shown). The polarized mitochondria were originally localized in the perinuclear area of the cells represented by the void space when loaded with calcein-AM as indicated by an arrow in Fig. 5B. However, the mitochondria were rather diffuse and obscured in the round cells, suggesting increased mitochondrial membrane permeability or damage in these cells (Fig. 5B and D). In the presence of UDCA for 48 hours, the number of round cells significantly increased ($P < 0.005$) when compared with those treated with SN-38 alone, and an abundant number of apoptotic bodies were detected (see arrow in SN-38 + UDCA; Fig. 5D). UDCA alone did not induce any significant mitochondrial or cell volume changes (data not shown). The percentage of the round cells after 48-hour incubation was quantified in Fig. 5E. After 48 hours, SN-38 increased the number of round cells from ~3% to ~19%. Furthermore, the addition of 100 μmol/L UDCA resulted in an increased number of round cells to ~48% (Fig. 5E). The number of round cells determined 24 hours following

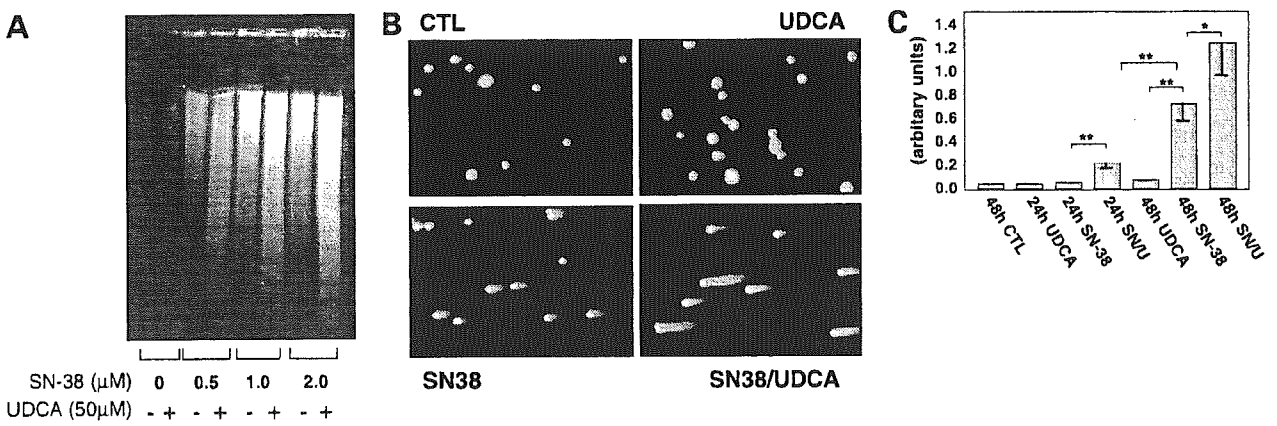

Figure 4. Induction of DNA fragmentation by SN-38 and UDCA. **A**, HT-29 cells were incubated with SN-38 for 2 h, washed with PBS thrice, and then further incubated in the presence or absence of 50 μmol/L UDCA for 72 h. Cells were collected and electrophoresed in 0.5% agarose gels. **B**, cells were incubated with 1 μmol/L SN-38 for 2 h and with 100 μmol/L UDCA for either 24 or 48 h after removal of SN-38. The cells loaded on low melting point agarose gels were permeabilized after solidification of the gel. Fragmented nucleic DNA migrates according to the molecular size. **C**, fluorescence intensity of these comets was visualized with a Meridian laser spectrometer, and the ratio of the tail over the head of the comet was calculated as described in Materials and Methods. Representative of three independent experiments. *, $P < 0.005$; **, $P < 0.05$, significantly different from respective control.

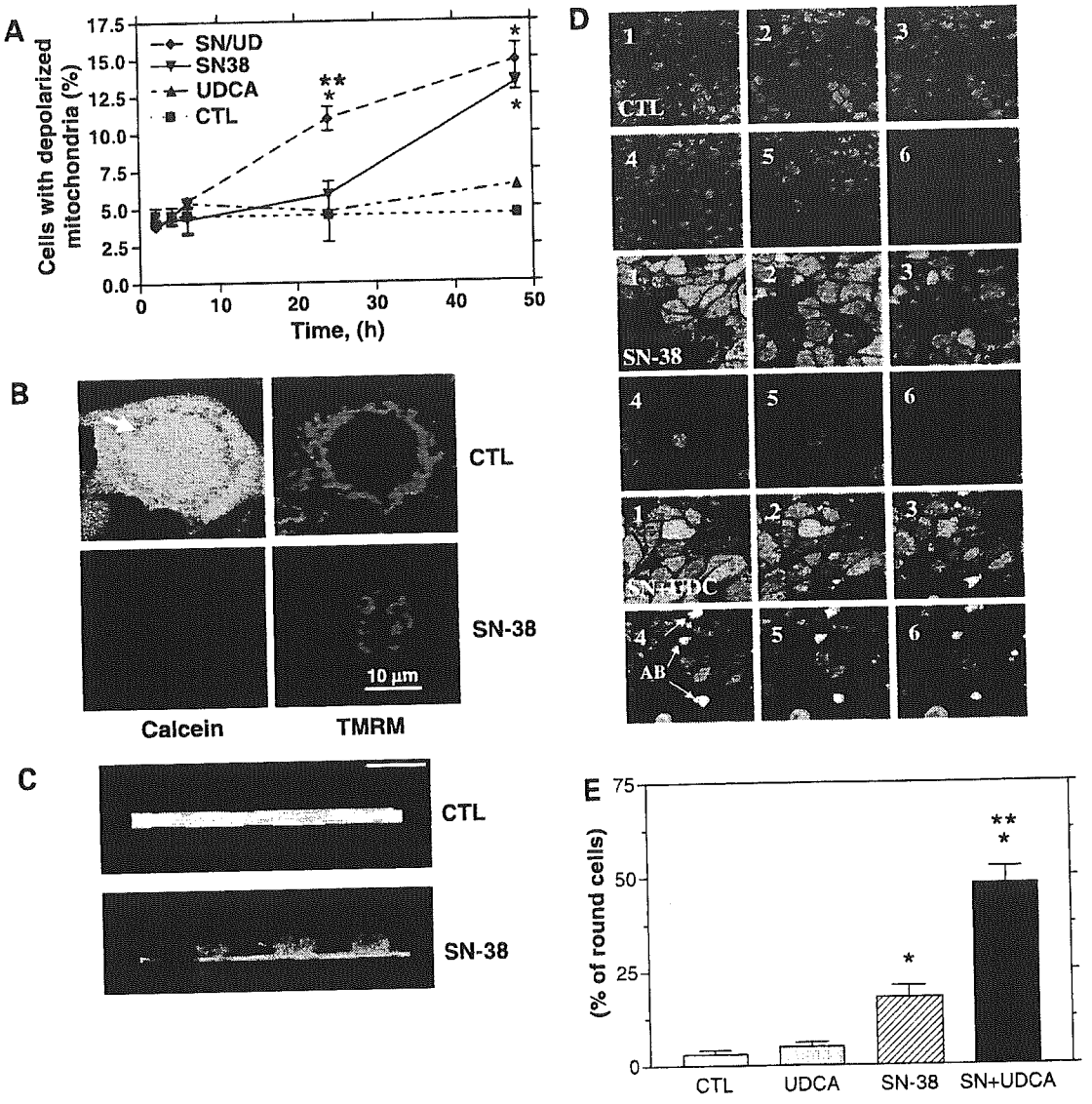

Figure 5. Reduction of $\Delta\Psi_m$ and mitochondrial membrane permeability transition by SN-38 and UDCA. **A,** $\Delta\Psi_m$ was determined by flow cytometry using the fluorescent marker JC-1. HT-29 cells were treated with 0.5 μmol/L SN-38 for 2 h, washed with PBS, and then incubated up to 48 h in the presence (*SN/UD*) and absence (*SN38*) of 100 μmol/L UDCA. After trypsinization, JC-1 was loaded into HT-29 cells and analyzed by flow cytometry. Depolarized mitochondria formed aggregates and this aggregation resulted in the alteration in fluorescent emission wavelength (525 - 590 nm). The number of cells with depolarized mitochondria was counted and expressed as percentage of control. **B,** HT-29 cells were treated as described above. For the final 20 min of incubation, the cells were coloaded with calcein-AM (1 μmol/L) and TMRM (0.5 μmol/L). Representative images of the HT-29 cells loaded with either calcein-AM or TMRM before and after SN-38 treatment. **C,** HT-29 cells costained with calcein-AM and TMRM were scanned under confocal laser scanning microscope and a three-dimensional image was reconstructed from the images of serial scanning. *CTL,* untreated control cells; *SN-38,* HT-29 cells 48 h after incubation with 0.5 μmol/L SN-38 for 2 h. **D,** HT-29 cells were incubated, loaded, and scanned as described above. *SN + UDC,* SN-38 + UDCA condition; *1-6,* serial confocal images collected as the focal plane was advanced in 0.2 μmol/L increments from the bottom of the cell layer. **E,** quantification of the rounded cells in SN-38-treated HT-29 cells. The number of rounded HT-29 cells was counted and expressed as percentage of total. In each group, total number of counted cells was 150 to 200. All the images were collected using a ×63 objective oil immersion lens in an inverted microscope. *Columns,* mean of two independent experiments done in duplicate; *bars,* SE. *, $P < 0.005$, significantly different from control; **, $P < 0.05$, significantly different from SN-38-treated cells.

SN-38 treatment was not significantly different from that of control, whereas the addition of UDCA for 24 hours after SN-38 removal resulted in a significantly increased number of round cells (data not shown). These results are consistent with the reduction of $\Delta\Psi_m$ by the combination of SN-38 and UDCA (Fig. 5A), suggesting a further alteration of the mitochondrial membrane permeability transition by the combination of SN-38 and UDCA. As a positive control for mitochondrial membrane depolarization, we treated the cells with increasing concentrations of FCCP, an inhibitor

of the mitochondrial oxidative chain. There was no increase in round cells, whereas the cells showed a diffuse pattern of depolarized mitochondria (data not shown). Therefore, the semidetachment of the cells is a phenomenon induced by SN-38 independently of its damaging effect on mitochondria alone.

Role of Caspase-3, Caspase-8, and Caspase-9 on the Combined Apoptotic Effect of SN-38 and UDCA

To test the hypothesis that UDCA activates the mitochondrial apoptotic pathway, we determined the caspase activities in treated HT-29 cells. As shown in Fig. 6A, SN-38 induced a significant activation of caspase-3 and caspase-8. The caspase-9 activity was slightly elevated by SN-38 alone but was not statistically significant. The addition of 100 μmol/L UDCA for 24 hours resulted in the further significant increase of both caspase-3 and caspase-9 activities without affecting that of caspase-8 (Fig. 6A).

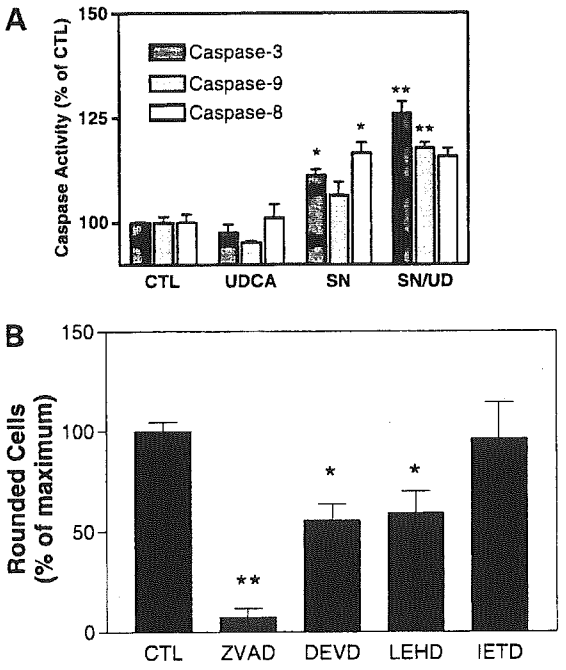

Figure 6. Role of caspases in the apoptotic effect of SN-38 + UDCA. **A,** HT-29 cells were incubated with 0.5 μmol/L SN-38 (*SN*) for 2 h. After removal of SN-38, the cells were further incubated with 100 μmol/L UDCA (*UD*). Caspase activity in the cell lysate of the treated cells was determined by colorimetric assay as described in Materials and Methods. *Columns,* mean percentage of control determined in the absence of both SN-38 and UDCA from two independent experiments done in duplicate; *bars,* SE. *, $P < 0.01$, significantly different from control; **, $P < 0.05$, significantly different from the condition with SN-38 alone. **B,** HT-29 cells were incubated with 0.5 μmol/L SN-38 for 2 h. After removal of SN-38, the cells were further incubated with 100 μmol/L UDCA in the presence of 20 μmol/L of various caspase inhibitors (*zVAD,* general caspase inhibitor; *DEVD,* caspase-3 inhibitor; *LEHD,* caspase-9 inhibitor; *IETD,* caspase-8 inhibitor) for 24 h. The number of round cells was assessed under each condition and expressed as percentage of maximum determined in the presence of SN-38 and UDCA and in the absence of the caspase inhibitors. The number of round cells determined in the presence of SN-38 alone was subtracted from that of SN-38 + UDCA. **, $P < 0.001$; * $P < 0.01$, significantly different from control.

Furthermore, the involvement of caspases in the UDCA-induced increased apoptotic effect of SN-38 was investigated using specific caspase inhibitors. The increased effect of UDCA on both SN-38-induced apoptosis and formation of round cells was almost completely abolished with 20 μmol/L of the general caspase inhibitor, ZVAD-fmk (Fig. 6B). The percentage of apoptotic cells induced by SN-38 followed with UDCA treatment for 24 hours was not significantly decreased in the presence of a specific caspase-8 inhibitor (IETD), whereas the incubation with either caspase-3 (DEVD) or caspase-9 (LEHD) inhibitor resulted in ~45% inhibition of the UDCA effect (Fig. 6B).

Role of JNK on the Combined Apoptotic Effect of SN-38 and UDCA

JNK is one of the MAPKs implicated in camptothecin-induced apoptosis. To investigate the possible involvement of the MAPKs in SN-38- and UDCA-induced apoptosis, the phosphorylation of ERK, p38, and JNK was determined by Western blotting using specific antibodies against the respective phosphorylated and total form of these kinases. These three kinases were phosphorylated to a certain extent even in untreated HT-29 cells. Following the addition of 0.5 μmol/L SN-38, the activation of ERK and p38 was observed as early as ~5 to 15 minutes and peaked at ~1 hour, whereas the phosphorylation of JNK was relatively delayed starting at ~30 minutes and reaching a plateau at ~2 hours (data not shown). This phosphorylation of JNK lasted for at least 6 hours after addition of SN-38 (Fig. 7A) and then gradually decreased over time to control level by 24 hours (Fig. 7B and C). In the simultaneous presence of SN-38 and 100 μmol/L UDCA, the phosphorylation level of JNK remained elevated at least up to 24 hours (Fig. 7B and C). Next, we used specific JNK (SP600125) and ERK (PD98059) inhibitors. These inhibitors almost completely inhibited JNK and ERK phosphorylation, respectively, as determined by Western blotting (Fig. 7C). Under these conditions, SP600125 prevented the potentiation of SN-38-induced apoptosis by UDCA (Fig. 7D). Taken together, the results of this study suggest that one of the key mechanisms by which UDCA increased SN-38-induced apoptosis includes enhanced and/or stabilization of JNK phosphorylation and activation.

Discussion

The present study shows that the bile acid, UDCA, promotes the apoptotic response induced by SN-38 not only in colon adenocarcinoma-derived HT-29 and LS174T cells but also in the hepatocarcinoma HepG2 cell line. Addition of concentrations ≥50 μmol/L UDCA after, rather than before or during, SN-38 administration increased DNA damage as well as decreased $\Delta\Psi_m$ resulting in an increased SN-38 induced apoptosis at least in HT-29 cells. UDCA had little apoptotic effect on its own; furthermore, under these conditions, UDCA did not affect the SN-38-induced alteration of the mRNA level of key proteins involved in either apoptotic or cell cycle pathways. Inhibition of caspase-3 and caspase-9 but not

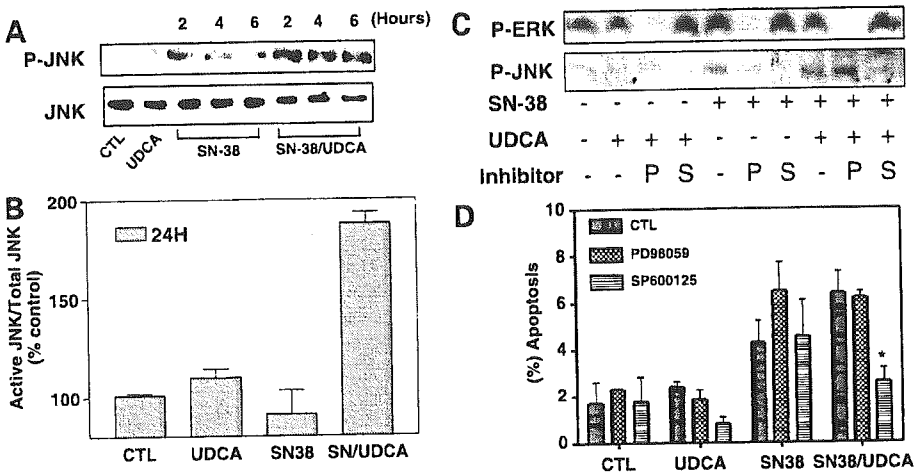

Figure 7. Role of JNK on the combined apoptotic effect of SN-38 and UDCA. **A**, HT-29 cells were incubated with 0.5 μmol/L SN-38 for 2 h. After removal of SN-38, the cells were further incubated without and with 100 μmol/L UDCA. Phosphorylated (*P-JNK*) and total (*JNK*) JNK expression was determined over time in the absence and presence of either SN-38 or SN-38 + UDCA. **B**, ratio between phosphorylated JNK and total JNK was calculated according to the densitometric analysis at 24 h. **C**, HT-29 cells were incubated in the presence of either 50 μmol/L PD98059 (*P*) or 25 μmol/L SP600125 (*S*) before the addition of 0.5 μmol/L SN-38. After removal of both the respective ERK and JNK inhibitors and SN-38, the cells were further incubated for 24 h with 100 μmol/L UDCA in the presence of the same respective inhibitor. The phosphorylation of ERK1/2 (*P-ERK*) and JNK was determined by Western blotting using specific anti-phosphorylated antibodies. Representative of three independent experiments. **D**, apoptotic cell death was determined by the morphologic identification of apoptotic cells by fluorescence microscopy using the conditions described in (*C*) and by using Hoechst 33258. * $P < 0.01$ compared with the same condition but without SP600125.

caspase-8 either partially or almost completely prevented the UDCA-induced apoptotic effect. These results contrast to reports supporting an antiapoptotic effect of UDCA against a variety of stimuli (15, 24). In these studies, the protective effect of this bile acid was attributed to the stabilization of the mitochondrial structure, thereby preventing the loss of cytochrome *c* (15, 25). Although there is no clear hypothesis to explain these differences, the present results are consistent with findings suggesting that UDCA enhances efficacy of photodynamic therapy on cancer cells (19). In the present study and that by Kessel et al., one of the clear effects of UDCA is to enhance the mitochondrial damage of the chemotherapeutic agents. Furthermore, the activation of JNK could be one of the reasons for our observed significant effect of UDCA when present after SN-38 exposure, whereas Kessel et al. reported the requirement for UDCA to be present before photoirradiation (19).

Apoptosis and necrosis can be distinguished morphologically (26). The common apoptotic markers, such as chromatin condensation, DNA fragmentation, apoptotic bodies, and caspase activation, are absent in necrotic cells (27). Once the apoptotic signal has been induced, the cell is rapidly cleared by phagocytosis without spilling its intracellular content. However, when apoptotic cells escape clearance, which is mostly the case in cell culture, the cells may present a loss of membrane permeability associated with late-stage apoptosis (termed secondary necrosis; ref. 28). Therefore, one of the possible mechanisms to explain the increased apoptosis and reduced necrosis in the presence of SN-38 and UDCA includes the UDCA-induced alteration of the apoptotic process and secondary necrosis formation. Indeed, UDCA could be preventing this loss in membrane permeability observed in secondary necrosis, because this bile acid has been shown to protect membranes against damage by hydrophobic and more toxic bile acids (29). However, the significant further decrease in colony growth observed in the presence of SN-38 and UDCA would rule against this hypothesis.

The observations using confocal laser scanning microscopy revealed the process of SN-38-induced apoptotic cell death and its enhancement by UDCA in HT-29 cells. Our results indicated that the detachment of the cells from the culture plate is an early event in apoptosis, which is consistent with previous reports using various colonic adenoma cell lines (30). In the presence of SN-38 and UDCA, the majority of the floating cells were externalizing phosphatidylserine, whereas <3% of the attached cells were phosphatidylserine positive. Deprivation of the cells from anchoring to substrate leads to rapid cell death. This form of apoptosis has been termed anoikis. Gunthert et al. observed an early detachment of the HT-29 cells from the plate in Fas-induced apoptosis (31). In this report, the authors proposed the shedding of cell surface adhesion molecules, which occurred at an early stage of Fas-dependent apoptosis, contributed to the active disintegration of the cells. However, the induction of the disappearance of these cell surface adhesion proteins may not be a Fas-specific phenomenon and may be induced by SN-38 and potentiated by UDCA.

Shrinkage of the cells, which is also generally considered as an early morphologic change in the apoptotic process, was not observed in the present study. In fact, most of

the cells treated with either SN-38 or SN-38 and UDCA showed an increased cell volume, which was independent of the cell density. This precludes the possibility that the increase in size is due to the death of the surrounding cells and the increased space availability. However, although the number of semidetached cells and apoptotic bodies was increased, this increase in cell volume with SN-38 was not modified by UDCA. These data support the likelihood that the blockade of the cell cycle in the S and G_2-M phases by SN-38 was responsible for the increase in cell volume as suggested previously (9). This is also consistent with the lack of effect of UDCA on SN-38-induced cell cycle alteration reported in the present study.

Release of cytochrome *c* from the mitochondria into the cytosol results in the activation of the caspase adaptor Apaf-1 and procaspase-9, which form a holoenzyme complex termed "apoptosome." Caspase-9 in context with this holoenzyme activates downstream caspases, most importantly caspase-3, which results in DNA fragmentation and apoptosis (32–34). In addition, the direct oligomerization of the Fas receptor (CD95/Apo-1) leads to the initial activation of the caspase cascade starting from caspase-8 (35). Recent reports indicated that bile acids can induce hepatocyte cell death via ligand-independent oligomerization of Fas and activation of the death receptor pathways (36). In addition, certain bile acids have been shown to activate a phosphatidylinositol 3-kinase/protein kinase Cζ/nuclear factor-κB survival pathway (37). This latter activation can oppose the Fas-dependent apoptosis and therefore can inhibit the inherent cytotoxicity of bile acids. The present study supports the involvement of caspase-9 rather than caspase-8 in the UDCA-induced potentiation of SN-38-induced apoptosis, because (*a*) the SN-38-induced caspase-3/9 activity is facilitated by UDCA and (*b*) a specific caspase-9 but not caspase-8 inhibitor can, at least partially, reduce the UDCA effect. These findings suggest the simultaneous activation of various apoptotic pathways by SN-38, whereas the involvement of UDCA is mostly limited to the caspase-9-dependent pathway. Taken together, the present study suggests that the effect of UDCA is correlated with mitochondrial membrane depolarization, and the promotion of the apoptotic signaling damage induced by SN-38, and is most probably independent from the Fas-associated apoptotic process.

SN-38 is the most potent metabolite of CPT-11 and thought to be a major player in the antitumor action of CPT-11 (6). It is known that the inhibition of DNA topoisomerase I by SN-38 leads to apoptotic cell death in various cell lines, including the adenocarcinoma LS174T colon cancer and hepatocellular HepG2 cell lines (7). The fact that SN-38 decreases the mRNA expression level of the antiapoptotic protein Bcl-x_L but not that of either Bcl-2 or Bax is of interest because it has been reported previously that 10-hydroxycamptothecin induced apoptosis in HepG2 cells by decreasing Bcl-2 and Bax (38). The results of the present study are more in line with those of Magrini et al. who have shown that CPT-11 decreased Bcl-x_L protein expression level without affecting that of both Bcl-2 and Bax in colonic HCT116 $p53^{-/-}$ cells (10). These authors suggested that the decrease in Bcl-x_L, known to inhibit Bax resulted in the integration of the liberated Bax into the mitochondrial membrane and the apoptosis induction (10). It is also worthwhile to mention that SN-38 induced a decreased mRNA expression level of $p16^{INKA}$ and c-fos. Indeed, in a previous study, Fukuoka et al. have reported that the apoptotic effect of CPT-11 was p16 dependent and was increased in A549 cells transfected with p16 (39). There are only a few studies that have focused on CPT-11 and c-fos. The study by Singh et al. suggests that there is an improved patient survival when c-fos expression is high (40). Therefore, the level of expression of both p16 and c-fos may have an important role in cells refractory to CPT-11, and further study of the role of these proteins in the CPT-11-induced cell death should be worthwhile. The stimulatory effect of various bile acids on c-fos mRNA expression and the lack thereof of UDCA has been reported previously (41) and is supported by results of the present study. Furthermore, the complete lack of effect of UDCA on the alteration of any of these mRNA levels supports a post-transcriptional effect of this bile acid.

The proapoptotic role of prolonged JNK activation has been reported recently in various colonic cancer cell lines, including HT-29 (42–44). Indeed, studies using target gene disruption have established that the JNK signaling pathway is required for stress-induced release of mitochondrial cytochrome *c* and apoptosis (43). Previous reports also revealed the activation of JNK by several chemopreventive agents, including SN-38, facilitating apoptosis in cancer cells (42, 44, 45). The intermediate signaling moiety between JNK activation and cytochrome *c* release may be linked to the Bax protein, as activated JNK fails to induce apoptosis in cells deficient of members of the proapoptotic Bax subfamily of the Bcl-2-related proteins. In the present study, the SN-38-induced JNK activation was further prolonged by the presence of UDCA, and pretreatment with SP600125, a specific JNK inhibitor, led to a substantial decrease in apoptotic cell death induced by SN-38 and UDCA. These findings suggest that the JNK pathway plays a pivotal role in SN-38- and UDCA-induced cell death. JNK phosphorylation by UDCA may not occur only after SN-38 stimulation but rather through a direct mechanism because the long-term incubation with UDCA alone also induces the JNK phosphorylation to a certain extent. It should also be noted that the simultaneous phosphorylation of all three major MAPK (JNK, ERK, and p38) pathways, which have different and, in some cases, opposite biological functions, suggests that the balance and integration of the MAPK pathways may modulate the commitment of the cells to either apoptosis or survival following external stimuli. Indeed, the extensive interaction among all three MAPKs has been reported in various tissues and cells and is relevant to cancer therapy (see ref. 46 for review). In the present study, JNK phosphorylation by SN-38 plus UDCA was further increased in the presence of an ERK inhibitor supporting the presence of cross-talk between these two pathways in HT-29 cells and the predominance of JNK-induced cell death when stimulated with SN-38 plus UDCA. It is possible that SN-38 can

induce simultaneous JNK and ERK phosphorylation and the balance between these two pathways determines the final fate of the cell. UDCA facilitation of JNK phosphorylation may in turn tip the balance between these pathways over time and enhance apoptosis.

In man, the biliary bile acid concentration ranges from 5 to 40 mmol/L, whereas the portal and systemic bile acid concentration ranges from 30 to 100 and 1 to 3 μmol/L, respectively. The oral administration of 150 to 600 mg UDCA (0.38–1.53 mmol) results in a significant increased UDCA concentration representing >50% of the total biliary bile acid concentration (47) and reaches a peak plasma concentration of up to 16 μmol/L in healthy volunteers (48). Furthermore, although the majority of the bile acid pool is reabsorbed from the small intestine, >5% escape the enterohepatic circulation and are found in the colon and feces. Therefore, although difficult to assess with accuracy, one could expect to see UDCA concentrations of 0.1 to 1 mmol/L in the colon. However, the bile acid can be dehydroxylated by bacterial enzymes, which would further decrease the intestinal UDCA concentration. To this effect, Makino and Nakagawa have reported that although UDCA was still detectable in the feces a large portion had been 7β-dehydroxylated to lithocholic acid (49). In addition, it is quite possible that the colonic UDCA concentration could be significantly increased if this bile acid was administered rectally. Together, these results support the possibility of achieving UDCA concentrations, from the combined apical and basolateral poles of the colonocytes following UDCA administration, as shown in the present study to be able to stimulate SN-38-induced apoptosis. Furthermore, it is worthwhile mentioning that, as previously shown clinically by Takeda et al., oral administration of UDCA, at least when combined with magnesium oxide and bicarbonate, did not increase the overall toxicity of CP-11/SN-38 (50).

In summary, UDCA increases the apoptotic and decreases the necrotic effects of SN-38 in the various adenocarcinoma cell lines, including HT-29. This effect of UDCA involves mitochondrial membrane depolarization and activation of caspase-3 and caspase-9 and these actions are mediated, at least in part, through JNK activation. Taken together, these results support a beneficial effect of UDCA by increasing the targeted apoptotic-associated cell death. By facilitating apoptosis over necrosis, UDCA could be preventing or at least decreasing the associated inflammatory response as well as facilitating wound healing. However, the clinical relevance of UDCA as an enhancer of chemotherapeutic lethality remains to be confirmed.

References

1. Kudoh S, Fujiwara Y, Takada Y, et al. Phase II study of irinotecan combined with cisplatin in patients with previously untreated small-cell lung cancer. West Japan Lung Cancer Group. J Clin Oncol 1998;16:1068–74.

2. Irvin WP, Price FV, Bailey H, et al. A phase II study of irinotecan (CPT-11) in patients with advanced squamous cell carcinoma of the cervix. Cancer 1998;82:328–33.

3. Shimizu Y, Umezawa S, Hasumi K. Successful treatment of clear cell adenocarcinoma of the ovary (OCCA) with a combination of CPT-11 and mitomycin C. Gan To Kagaku Ryoho 1996;23:587–93.

4. Ota K, Ohno R, Shirakawa S, et al. Late phase II clinical study of irinotecan hydrochloride (CPT-11) in the treatment of malignant lymphoma and acute leukemia. The CPT-11 Research Group for Hematological Malignancies. Gan To Kagaku Ryoho 1994;21:1047–55.

5. Rivory LP, Bowles MR, Robert J, Pond SM. Conversion of irinotecan (CPT-11) to its active metabolite, 7-ethyl-10-hydroxycamptothecin (SN-38), by human liver carboxylesterase. Biochem Pharmacol 1996;52:1103–11.

6. Kawato Y, Aonuma M, Hirota Y, Kuga H, Sato K. Intracellular roles of SN-38, a metabolite of the camptothecin derivative CPT-11, in the antitumor effect of CPT-11. Cancer Res 1991;51:4187–91.

7. Morris EJ, Geller HM. Induction of neuronal apoptosis by camptothecin, an inhibitor of DNA topoisomerase-I: evidence for cell cycle-independent toxicity. J Cell Biol 1996;134:757–70.

8. Whitacre CM, Zborowska E, Willson JK, Berger NA. Detection of poly(ADP-ribose) polymerase cleavage in response to treatment with topoisomerase I inhibitors: a potential surrogate end point to assess treatment effectiveness. Clin Cancer Res 1999;5:665–72.

9. Ikegami T, Ha L, Arimori K, et al. Intestinal alkalization as a possible preventive mechanism in irinotecan (CPT-11)-induced diarrhea. Cancer Res 2002;62:179–87.

10. Magrini R, Bhonde MR, Hanski ML, et al. Cellular effects of CPT-11 on colon carcinoma cells: dependence on p53 and hMLH1 status. Int J Cancer 2002;101:23–31.

11. Li TK, Liu LF. Tumor cell death induced by topoisomerase-targeting drugs. Annu Rev Pharmacol Toxicol 2001;41:53–77.

12. Pisani P, Parkin DM, Bray F, Ferlay J. Estimates of the worldwide mortality from 25 cancers in 1990. Int J Cancer 1999;83:18–29.

13. Hague A, Elder DJ, Hicks DJ, Paraskeva C. Apoptosis in colorectal tumour cells: induction by the short chain fatty acids butyrate, propionate and acetate and by the bile salt deoxycholate. Int J Cancer 1995;60:400–6.

14. Garewal H, Bernstein H, Bernstein C, Sampliner R, Payne C. Reduced bile acid-induced apoptosis in "normal" colorectal mucosa: a potential biological marker for cancer risk. Cancer Res 1996;56:1480–3.

15. Rodrigues CM, Fan G, Ma X, Kren BT, Steer CJ. A novel role for ursodeoxycholic acid in inhibiting apoptosis by modulating mitochondrial membrane perturbation. J Clin Invest 1998;101:2790–9.

16. Botla R, Spivey JR, Aguilar H, Bronk SF, Gores GJ. Ursodeoxycholate (UDCA) inhibits the mitochondrial membrane permeability transition induced by glycochenodeoxycholate: a mechanism of UDCA cytoprotection. J Pharmacol Exp Ther 1995;272:930–8.

17. Jiang X, Wang X. Cytochrome *c* promotes caspase-9 activation by inducing nucleotide binding to Apaf-1. J Biol Chem 2000;275:31199–203.

18. Du C, Fang M, Li Y, Li L, Wang X. Smac, a mitochondrial protein that promotes cytochrome *c*-dependent caspase activation by eliminating IAP inhibition. Cell 2000;102:33–42.

19. Kessel D, Caruso JA, Reiners JJ, Jr. Potentiation of photodynamic therapy by ursodeoxycholic acid. Cancer Res 2000;60:6985–8.

20. Schlottman K, Wachs FP, Krieg RC, Kullmann F, Scholmerich J, Rogler G. Characterization of bile salt-induced apoptosis in colon cancer cell lines. Cancer Res 2000;60:4270–6.

21. Qiao L, Yacoub A, Studer E, et al. Inhibition of the MAPK and PI3K pathways enhances UDCA-induced apoptosis in primary rodent hepatocytes. Hepatology 2002;35:779–89.

22. Nieminen AL, Saylor AK, Tesfai SA, Herman B, Lemasters JJ. Contribution of the mitochondrial permeability transition to lethal injury after exposure of hepatocytes to *t*-butylhydroperoxide. Biochem J 1995;307:99–106.

23. Laemmli UK. Cleavage of structural proteins during the assembly of the head of bacteriophage T4. Nature (Lond) 1970;227:680–5.

24. Neuman MG, Shear NH, Bellentani S, Tiribelli C. Role of cytokines in ethanol-induced cytotoxicity *in vitro* in Hep G2 cells. Gastroenterology 1998;115:157–66.

25. Rodrigues CM, Ma X, Linehan-Stieers C, Fan G, Kren BT, Steer CJ. Ursodeoxycholic acid prevents cytochrome *c* release in apoptosis by inhibiting mitochondrial membrane depolarization and channel formation. Cell Death Differ 1999;6:842–54.

26. Majno G, Joris I. Apoptosis, oncosis, and necrosis. An overview of cell death. Am J Pathol 1995;146:3 - 15.

27. Bonfoco E, Krainc D, Ankarcrona M, Nicotera P, Lipton SA. Apoptosis and necrosis: two distinct events induced, respectively, by mild and intense insults with *N*-methyl-D-aspartate or nitric oxide/superoxide in cortical cell cultures. Proc Natl Acad Sci U S A 1995;92:7162 - 6.

28. Wu X, Molinaro C, Johnson N, Casiano CA. Secondary necrosis is a source of proteolytically modified forms of specific intracellular autoantigens: implications for systemic autoimmunity. Arthritis Rheum 2001;44: 2642 - 52.

29. Guldutuna S, Zimmer G, Imhof M, Bhatti S, You T, Leuschner U. Molecular aspects of membrane stabilization by ursodeoxycholate [see comment]. Gastroenterology 1993;104:1736 - 44.

30. Hague A, Manning AM, Hanlon KA, Huschtscha LI, Hart D, Paraskeva C. Sodium butyrate induces apoptosis in human colonic tumour cell lines in a p53-independent pathway: implications for the possible role of dietary fibre in the prevention of large-bowel cancer. Int J Cancer 1993;55:498 - 505.

31. Gunthert AR, Strater J, von Reyher U, et al. Early detachment of colon carcinoma cells during CD95(APO-1/Fas)-mediated apoptosis. I. Deadhesion from hyaluronate by shedding of CD44. J Cell Biol 1996;134: 1089 - 96.

32. Deveraux QL, Roy N, Stennicke HR, et al. IAPs block apoptotic events induced by caspase-8 and cytochrome *c* by direct inhibition of distinct caspases. EMBO J 1998;17:2215 - 23.

33. Slee EA, Harte MT, Kluck RM, et al. Ordering the cytochrome *c*-initiated caspase cascade: hierarchical activation of caspases-2, -3, -6, -7, -8, and -10 in a caspase-9-dependent manner. J Cell Biol 1999;144:281 - 92.

34. Sun XM, MacFarlane M, Zhuang J, Wolf BB, Green DR, Cohen GM. Distinct caspase cascades are initiated in receptor-mediated and chemical-induced apoptosis. J Biol Chem 1999;274:5053 - 60.

35. Muzio M, Chinnaiyan AM, Kischkel FC, et al. FLICE, a novel FADD-homologous ICE/CED-3-like protease, is recruited to the CD95 (Fas/APO-1) death-inducing signaling complex. Cell 1996;85:817 - 27.

36. Faubion WA, Guicciardi ME, Miyoshi H, et al. Toxic bile salts induce rodent hepatocyte apoptosis via direct activation of Fas. J Clin Invest 1999;103:137 - 45.

37. Rust C, Karnitz LM, Paya CV, Moscat J, Simari RD, Gores GJ. The bile acid taurochenodeoxycholate activates a phosphatidylinositol 3-kinase-dependent survival signaling cascade. J Biol Chem 2000;275:20210 - 6.

38. Zhang XW, Xu B. Differential regulation of p53, c-Myc, Bcl-2, Bax and AFP protein expression, and caspase activity during 10-hydroxycamptothecin-induced apoptosis in Hep G2 cells. Anticancer Drugs 2000;11: 747 - 56.

39. Fukuoka K, Nishio K, Fukumoto H, et al. Ectopic p16(ink4) expression enhances CPT-11-induced apoptosis through increased delay in S-phase progression in human non-small-cell-lung-cancer cells. Int J Cancer 2000; 86:197 - 203.

40. Singh A, Tong A, Ognoskie N, Meyer W, Nemunaitis J. Improved survival in patients with advanced colorectal carcinoma failing 5-fluorouracil who received irinotecan hydrochloride and have high intratumor c-fos expression. Am J Clin Oncol 1998;21:466 - 9.

41. Di Toro R, Campana G, Murari G, Spampinato S. Effects of specific bile acids on c-fos messenger RNA levels in human colon carcinoma Caco-2 cells. Eur J Pharm Sci 2000;11:291 - 8.

42. Chen C, Shen G, Hebbar V, Hu R, Owuor ED, Kong AN. Epigallocatechin-3-gallate-induced stress signals in HT-29 human colon adenocarcinoma cells. Carcinogenesis 2003;24:1369 - 78.

43. Tournier C, Hess P, Yang DD, et al. Requirement of JNK for stress-induced activation of the cytochrome *c*-mediated death pathway. Science 2000;288:870 - 4.

44. Somasundaram S, Edmund NA, Moore DT, Small GW, Shi YY, Orlowski RZ. Dietary curcumin inhibits chemotherapy-induced apoptosis in models of human breast cancer. Cancer Res 2002;62:3868 - 75.

45. Costa-Pereira AP, McKenna SL, Cotter TG. Activation of SAPK/JNK by camptothecin sensitizes androgen-independent prostate cancer cells to Fas-induced apoptosis. Br J Cancer 2000;82:1827 - 34.

46. Kyriakis JM, Avruch J. Mammalian mitogen-activated protein kinase signal transduction pathways activated by stress and inflammation. Physiol Rev 2001;81:807 - 69.

47. Lindblad L, Lundholm K, Schersten T. Bile acid concentrations in systemic and portal serum in presumably normal man and in cholestatic and cirrhotic conditions. Scand J Gastroenterol 1977;12:395 - 400.

48. Setchell KD, Rodrigues CM, Podda M, Crosignani A. Metabolism of orally administered tauroursodeoxycholic acid in patients with primary biliary cirrhosis. Gut 1996;38:439 - 46.

49. Makino I, Nakagawa S. Changes in biliary lipid and biliary bile acid composition in patients after administration of ursodeoxycholic acid. J Lipid Res 1978;19:723 - 8.

50. Takeda Y, Kobayashi K, Akiyama Y, et al. Prevention of irinotecan (CPT-11)-induced diarrhea by oral alkalization combined with control of defecation in cancer patients. Int J Cancer 2001;92:269 - 75.

Proton Beam Therapy for Hepatocellular Carcinoma: A Retrospective Review of 162 Patients

Toshiya Chiba,[1] Koichi Tokuuye,[2] Yasushi Matsuzaki,[1] Shinji Sugahara,[2] Yoshimichi Chuganji,[1] Kenji Kagei,[2] Junichi Shoda,[1] Masaharu Hata,[2] Masato Abei,[1] Hiroshi Igaki,[2] Naomi Tanaka,[1] and Yasuyuki Akine[2]

Abstract **Purpose:** We present results of patients with hepatocellular carcinoma (HCC) treated with proton beam therapy.

Experimental Design: We reviewed 162 patients having 192 HCCs treated from November 1985 to July 1998 by proton beam therapy with or without transarterial embolization and percutaneous ethanol injection. The patients in the present series were considered unsuitable for surgery for various reasons, including hepatic dysfunction, multiple tumors, recurrence after surgical resection, and concomitant illnesses. The median total dose of proton irradiation was 72 Gy in 16 fractions over 29 days.

Results: The overall survival rate for all of the 162 patients was 23.5% at 5 years. The local control rate at 5 years was 86.9% for all 192 tumors among the 162 patients. The degree of impairment of hepatic functions attributable to coexisting liver cirrhosis and the number of tumors in the liver significantly affected patient survival. For 50 patients having least impaired hepatic functions and a solitary tumor, the survival rate at 5 years was 53.5%. The patients had very few acute reactions to treatments and a few late sequelae during and after the treatments.

Conclusions: Proton beam therapy for patients with HCC is effective, safe, well tolerable, and repeatable. It is the useful treatment mode for either cure or palliation for patients with HCC irrespective of tumor size, tumor location in the liver, insufficient feeding of the tumor with arteries, presence of vascular invasion, impaired hepatic functions, and coexisting intercurrent diseases.

The estimated number of patients with primary hepatocellular carcinoma (HCC) was ~1 million per year worldwide (1); the average survival for patients with HCC is a few months when untreated (2–4). In Japan, HCC is the third highest cause of cancer-related deaths for men and the fourth for women (5). Patients having long-term hepatitis B or C with liver cirrhosis are frequently found to have HCC; 90% of patients with HCC have had hepatitis C virus infection (6, 7).

Several treatment modalities are currently available for patients with HCC. For 17,885 patients with HCC treated in Japan over the 2-year period (8) from January 1998 to December 1999, proportions of patients with HCC treated with each modality were 51.4% for transarterial chemoembolization (9–13), 42.1% for transcatheter arterial embolization, 29.2% for surgery (14) 25.7% for percutaneous ethanol injection (15, 16), 7.3% for microwave coagulation therapy (17, 18), 2.1% for radiofrequency ablation (19–21), and 1.5% for radiotherapy.

Photon therapy has rarely been used in HCC treatment because the tolerance dose is ~30 Gy per 3 weeks when the entire organ is irradiated, which is considerably lower than that necessary for tumor control (22–26).

Proton beams allow a rapidly increasing dose at the end of the beam range (Bragg peak) with which excellent dose localization to the target is obtained (27). We began proton beam therapy for malignancies of various organs, including the liver, in 1983 (28). We previously reported excellent local tumor controls in patients with HCCs treated with proton beam therapy (26, 28–31). In this report, we present long-term results of proton beam therapy for 162 patients having 192 HCCs treated from 1985 to 1998.

Patients And Methods

Patients. The present study was conducted according to the Helsinki Declaration and approved by the Ethics Committee of the University of Tsukuba. All patients gave their written informed consents.

Patients with at least one of following conditions were eligible for proton beam therapy: (*a*) medically inoperable conditions attributable to coexisting advanced cirrhosis (i.e., indocyanin green R_{15} > 25%, serum total bilirubin level 34.2-59.9 μmol/L) and other intercurrent diseases; (*b*) HCC(s) not suitable for surgical resection and considered difficult to control with nonsurgical treatments, such as transcatheter

Authors' Affiliations: Departments of [1]Gastroenterology and [2]Radiation Oncology, Institute of Clinical Medicine, University of Tsukuba, Ibaraki, Japan

Received 7/9/04; revised 10/28/04; accepted 12/20/04.

Grant support: Grant-in-Aid for Cancer Research (15-9) and Second Term Comprehensive 10-Year Strategy for Cancer Control (H-15-006) from the Ministry of Health, Labour, and Welfare of the Japanese Government.

The costs of publication of this article were defrayed in part by the payment of page charges. This article must therefore be hereby marked *advertisement* in accordance with 18 U.S.C. Section 1734 solely to indicate this fact.

Note: T. Chiba and K. Tokuuye contributed equally to this work. Presented in part at the 45th Annual Meeting of the American Society for Therapeutic Radiology and Oncology, October 2003, Salt Lake City, Utah.

Requests for reprints: Koichi Tokuuye, Radiation Oncology, Institute of Clinical Medicine, University of Tsukuba, Tennodai 1-1-1, Tsukuba, Ibaraki 305-8575, Japan. Phone: 81-29-853-7124; Fax: 81-29-853-7102; E-mail: ktokuue@pmrc.tsukuba.ac.jp.

arterial embolization and percutaneous ethanol injection; (*c*) patient's refusal of surgery. The patient was required to have three or fewer tumors in the liver to enter the study; when the patient had multiple tumors, they were encompassed in a single irradiation field.

From November 1985 to July 1998, we treated 165 patients with HCCs using proton beam therapy at the Proton Medical Research Center, University of Tsukuba. Three of the 165 patients were excluded from present analysis: one patient discontinued proton beam therapy because of severe cholecystitis not attributable to irradiation; one patient discontinued the treatment for nonmedical reasons; and one patient underwent liver transplantation following proton beam therapy. The remaining 162 patients having 192 HCCs were reviewed with regard to survival rates, local control rates, and treatment sequelae.

Of the 162 patients, 110 underwent ultrasound-guided percutaneous needle (21 Majima needle, Top Co., Ltd., Tokyo, Japan) biopsy, and 100 of the 110 were diagnosed pathologically as having HCC. The remaining 52 patients did not undergo needle biopsy for various reasons: tumor location was considered too dangerous for needle insertion, concomitant illness, and patient's refusal of biopsy. For 100 patients with pathologically diagnosed HCC, 95% of the patients had tumors of grade I and II in the Edmondson and Steiner grade (32). Thirty-nine of the 62 patients without pathologic diagnosis were judged to have HCC based on increased serum α-fetoprotein level of >100 μg/L and imaging studies. The remaining 23 patients were diagnosed solely on imaging studies.

Table 1 shows patient characteristics. The median age was 62.5 years ranging from 41 to 84 years. Patients were categorized retrospectively according to the degree of impairment in the hepatic function using Child-Pugh classification (33). About half of the patients showed class B and C in the classification. Of the patients, 86% had performance status 0 or 1.

Table 1. Clinical characteristics of patients

Characteristics	No. patients (%)
Age (y)	
<60	56 (34.6)
60-69	72 (44.4)
≥70	34 (21.0)
Gender	
Men	124 (76.5)
Women	38 (23.5)
Underlying liver disorders	
Cirrhosis	154 (95.1)
A	82 (50.6)
B	62 (38.3)
C	10 (6.2)
Chronic hepatitis	7 (4.3)
Normal liver	1 (0.6)
Etiology of liver disorders	
Hepatitis B virus	15 (9.3)
Hepatitis C virus	129 (79.6)
Hepatitis B and C viruses	3 (1.9)
Non – hepatitis B, non – hepatitis C	11 (6.8)
Alcoholic	2 (1.2)
Unknown	2 (1.2)
Performance status	
0	61 (37.7)
1	79 (48.8)
2	21 (13.0)
3	1 (0.6)
4	0 (0)

Table 2. Background of hepatic tumor at entry

Characteristics	*n* (%)
No. tumors	
Single	80 (49.4)
Multiple	82 (51.6)
Type of tumor	
Nodular	156 (96.3)
Massive	6 (3.7)
Diffuse	0
Tumor-node-metastasis stage	
I	66 (40.7)
II	70 (43.2)
IIIA	25 (15.4)
IIIB	1 (0.6)
Tumor size (cm)*	
<3.0	51 (26.6)
3.0-5.0	108 (56.3)
>5.0	33 (17.2)
Serum α-fetoprotein (μg/L)	
<20	50 (30.9)
20-99	38 (23.5)
100-500	35 (21.6)
>500	39 (24.1)

*192 tumors treated by proton beam therapy.

Table 2 shows characteristics of 162 tumors. Tumors were categorized retrospectively according to International Union Against Cancer tumor-node-metastasis classifications (34). Of the patients, 60% had advanced tumors (stages II and IIIB). Among the 25 patients with stage IIIA, 10 patients had tumors involving a major branch of the portal vein (portal vein tumor thrombus). Of those 10 patients, 6 had portal vein tumor thrombus in the main trunk. The median maximal diameter of tumors was 3.8 cm ranging from 1.5 to 14.5 cm. Of the 162 patients, 112 (69.1%) had ≥20 μg/L in serum α-fetoprotein levels for which the median value was 227 μg/L (range, 21-12,539 μg/L).

Proton Irradiation. Procedures for proton beam therapy at the University of Tsukuba were reported previously (28, 35). Briefly, proton beams were provided with a booster synchrotron of the High Energy and Accelerator Research Organization. The beam energy was degraded to 250 from 500 MeV before medical use. Proton beams were available for medical use for 4 hours a day on ~120 days a year. The two treatment rooms were equipped with either a horizontal or a vertical port. We irradiated patients once a day, 3 or 4 days a week because of the limited time for using the beam.

Fiducial markers (0.8 mm in diameter and 2 mm long iridium seeds) were implanted adjacent to the tumor under ultrasonography guidance. A clinical target volume was gross tumor volume plus 5 to 10 mm margins at each axial plane on the treatment planning computed tomography images. Irradiation was given mostly with right-angled vertical and horizontal beams. For patients who had a tumor adjacent to the gastrointestinal tract, we irradiated the patient with other angles whenever necessary to avoid irradiating the gastrointestinal tract. We started to use respiration-gated irradiation (36, 37) in December 1992 to reduce the irradiated volume attributable to organ motion that accompanies breathing.

Of the 192 tumors irradiated, 9 tumors were irradiated simultaneously, resulting in a total number of treatment courses of 183. Of the 162 patients, 11 had two courses of treatment at different times, 2 had three courses, and 2 had four courses. The median total dose was 72 Gy

ranging from 50 to 88 Gy with a median fraction dose being 4.5 Gy ranging from 2.9 to 6 Gy. Patients were treated with different fractionation regimens: 72 Gy in 16 fractions over 24 to 43 days for 64 treatment courses, 78 Gy in 20 fractions over 33 to 42 days for 11 courses, 84 Gy in 24 fractions over 33 to 50 days for 10 courses, 50 Gy in 10 fractions over 13 to 21 days for 10 courses, and miscellaneous regimens for the remaining 97 courses. Various fractionation regimens were used especially in the earlier period of the present study. For that reason, equivalent doses with 2 Gy per fraction were calculated using a linear quadratic model with α/β ratios of 10 and 3 for early and late responding tissues (Table 3; ref. 38).

Follow-up. After completion of proton beam therapy, patients were examined every 3 months until 2 or 3 years and every 6 months afterward. Follow-up examinations included the following whenever possible: clinical history; physical examination, including assessing performance status according to the WHO handbook for reporting results of cancer treatment (39); biochemical examination, serum α-fetoprotein values; abdominal computed tomography or magnetic resonance imaging; and percutaneous needle biopsy 3 weeks after the completion of irradiation.

Local tumor control was defined as the situation in which an irradiated tumor showed no sign of regrowing and no new tumor appearing in the treatment volume.

A patient was considered to have died of hepatic failure when the patient died with marked progression of coexisting liver cirrhosis without having marked growing of HCC. Death from tumor progression occurred when the patient died with marked growing of HCC (more than a half volume of the whole liver) and distant metastasis without displaying progressing liver cirrhosis.

Treatment Sequelae. An increase of serum total bilirubin >51.3 μmol/L was considered significant acute toxicity in the hepatic function. Decreases of >20 g/L hemoglobin, >3 × 10^9/L WBC, and >50 × 10^9/L platelet count were considered significant acute treatment sequelae in the hematopoietic systems. Late sequelae were graded retrospectively according to the late radiation morbidity scoring scheme of the Radiation Therapy Oncology Group/European Organization for Research and Treatment of Cancer (40).

Statistical Methods. Survival rates and local control rates were calculated with the Kaplan-Meier method (41). Statistical significance of differences for both survival rates and local control rates was examined using the log-rank test (42). The difference between the two values calculated was examined using Student's *t* test or Fisher's exact test. Possible factors affecting survival were assessed with Cox proportional hazards regression analysis (43). Statistical analyses were done with SPSS version 11.0 (SPSS, Inc., Chicago IL).

Results

Patients were followed up until death or June 30, 2003. The median observation period for survival for all patients was 31.7 months ranging from 3.1 to 133.2 months.

Table 3. Dose fractionations and equivalent doses when given 2 Gy per fraction

Total dose (Gy)	No. fractions	Dose/ fraction	Equivalent total doses (2 Gy/fraction) $\alpha/\beta = 10$	$\alpha/\beta = 3$
72	16	4.5	87.0	108.0
78	20	3.9	90.4	107.6
84	24	3.5	94.5	109.2
50	10	5.0	62.5	80.0

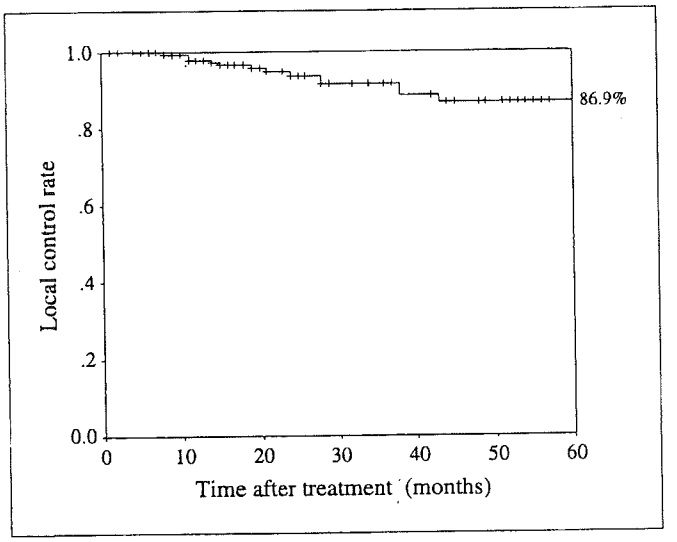

Fig. 1. Local tumor control after proton beam therapy.

Of the 162 patients, 17 were alive at their last follow-up. Their follow-up periods ranged from 32.4 to 133.2 months.

Imaging studies after proton beam therapy for four patients having four HCCs were unavailable; hence, the four patients were considered lost to follow-up for local control analysis at the end of treatment.

Local Tumor Control. The local control rate at 5 years was 86.9% for all of the 192 tumors among the 162 patients (Fig. 1). No significant difference in the local control rate at 5 years was observed between patients with tumors <5 cm in maximal diameter (87.8%) and those with >5 cm (82.1%; $P = 0.40$). Thirteen tumors locally recurred between 7 and 43 months (median, 21 months) after the completion of the irradiation. Maximal diameter of tumors that had recurred were median 4.7 cm ranging from 2.0 to 7.0 cm before irradiation. The tumors were irradiated to median total doses of 72 Gy ranging from 55 to 84 Gy. For locally controlled tumors, the maximal diameter was median 3.5 cm ranging from 1.5 to 14.5 cm and total doses irradiated were median 72 Gy ranging from 50 to 88 Gy. No correlation was found among local control and equivalent doses ($\alpha/\beta = 10$).

No significant difference in local control was observed between those treated with proton beam therapy with other modalities (90.7%) and those treated with proton beam therapy alone (81.3%; $P = 0.22$).

Eight of 68 (11.8%) tumors treated before December 1992, when we started respiratory-gated irradiation, recurred locally. In contrast, only 5 of 124 (4.0%) tumors treated after December 1992 recurred. Notwithstanding, that difference was not statistically significant ($P = 0.07$).

Survival. The overall survival rate for all of the 162 patients at 5 years was 23.5% (Fig. 2). The degree of impairment in the hepatic function attributable to coexisting cirrhosis and the number of tumors affected survival on the Cox regression analysis (Table 4). Tumor size, total irradiated dose given, and prior treatments before proton irradiation were not significant factors.

Survival rates for patients with chronic hepatitis and class A cirrhosis were significantly better than for those with B cirrhosis and those with C cirrhosis ($P < 0.0001$); no significant

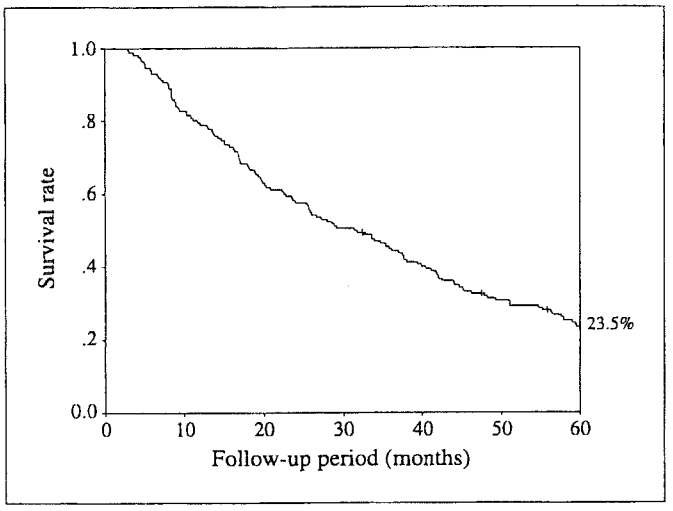

Fig. 2 Actual survival for all the patients.

difference was found between patients with B cirrhosis and those with C cirrhosis (Fig. 3).

Five-year survival rates according to the tumor-node-metastasis classification were as follows: 45.3% for stage I, 11.2% for stage II, and 26.9% for stage IIIA.

The 5-year survival rate for patients without prior therapy (45 patients) and those with prior therapy (117 patients) were 37.7% and 17.9% (P = 0.02), respectively.

There were 50 patients with favorable prognostic factors (Child-Pugh class A and solitary tumor) in the present series, and in these patients, the 5-year survival rate was 53.5% (Fig. 4).

Performance Status. Two (1.4%) patients were with performance status 0 before irradiation and performance status 1 after irradiation; another 2 (1.4%) patients were performance status 2 before and performance status 3 after irradiation. All remaining patients had stable performance status before and after irradiation.

Histopathologic Changes. Of the 100 patients who had been diagnosed pathologically as having HCC before irradiation, 47 were unable to undergo biopsy after the irradiation because the tumor was not detected with ultrasound. The remaining 53 patients with 53 tumors underwent biopsy 3 weeks after completion of proton beam therapy. Complete necrosis was observed in 12 (22.6%) tumors, degeneration of the nucleus and vessels in 16 (30.2%), fibrosis in 2 (3.8%), disappearance of tumor cells in 9 (17.0%), and no change in 14 (26.4%).

Vascular Invasion. Vascular invasion of the tumor or portal vein tumor thrombus into the main stem or the primary bifurcation of the portal vein was shown in 10 patients. The median total dose given to portal vein tumor thrombus was 55.3 Gy in 15 fractions over 20 days ranging from 50 Gy in 10 fractions over 13 days to 77 Gy in 22 fractions over 44 days. After irradiation, the tumors in the vessels were reduced in size markedly without impairing the patient's hepatic functions. The median survival period after proton beam therapy for the patients was 26.4 months ranging from 5.1 to 76 months.

Treatment Sequelae. Elevated plasma aspartate transaminase and alanine transaminase values by a factor of 3 at the most were observed in 18 patients on 18 courses (9.7%). However, they subsided quickly without causing any remarkable problems.

Table 5 shows that there were very few acute reactions to the treatment in 162 patients on 185 courses aside from the transient elevation of aspartate transaminase and alanine transaminase. All acute reactions subsided within 2 weeks. No patients discontinued treatment because of the acute reactions.

Five patients had late sequelae of grade II or higher: one patient had fibrotic stenosis of the common bile duct, which was located in the treatment volume, 13 months after irradiation; two patients had biloma with infection adjacent to the irradiated volume 29 and 38 months after irradiation, respectively; one patient had intractable gastric ulcer in the treatment volume 4 months after irradiation; the remaining patient had an ulcer in the ascending colon 6 months after irradiation. All patients who had developed late sequelae were treated before 1995. No patients died of treatment sequelae in the present series.

Outcome. As of June 2003, 145 of the 162 (89.5%) patients were dead. Of all 162 patients, 85% had developed another HCC(s) in the liver within 5 years following proton beam therapy. They underwent transarterial chemoembolization/transcatheter arterial embolization (51.4%), proton beam therapy (13.3%), percutaneous ethanol injection (6.7%), miscellaneous therapies, including systemic chemotherapy (6.7%), and no treatment (22.0%) as treatments for the newly developed HCCs.

Causes of death for the 145 patients were hepatic failure for 55 (37.9%) patients, 12 of whom had gastrointestinal bleeding at their death; tumor progression for 68 (46.9%); intercurrent diseases (renal failure for 4 patients, intracranial hemorrhage for 3, pneumonia for 3, and miscellaneous for 4) for 14 (9.7%); suicide for 1 (0.7%); and unknown for 7 (4.8%).

Table 4. Results of a Cox proportional hazards regression

Variable	Adjusted rate ratio (95% confidence interval of hazard ratio)	P
Child-Pugh classification		
A	1.00	
B*	2.22 (1.54-3.19)	<0.0001
C†	3.57 (1.81-7.03)	0.0002
No. tumors		
Solitary	1.00	
Multiple	1.58 (1.09-2.31)	0.02
Tumor size		
<50	1.00	
≥50	1.41 (0.92-2.15)	0.11
Proton doses		
<72	1.00	
≥72	1.01 (0.74-1.46)	0.95
Prior treatment		
Received	1.00	
Not received	0.88 (0.58-1.34)	0.56

*Child-Pugh B compared with those of Child-Pugh A.
†Child-Pugh C compared with those of Child-Pugh A.

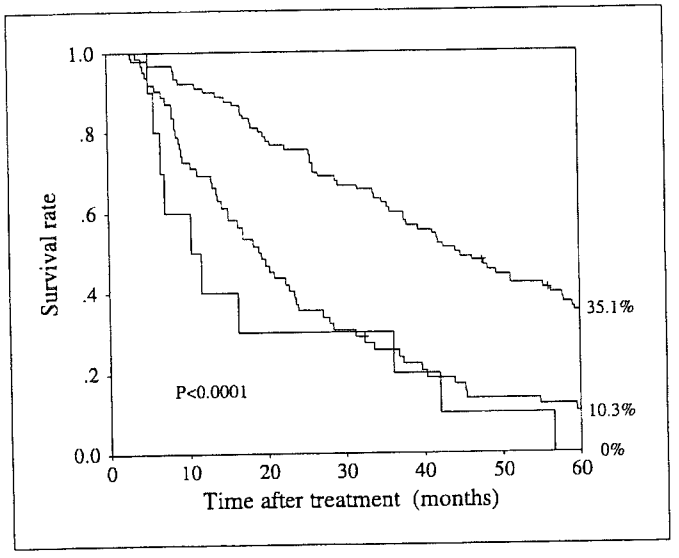

Fig. 3. Survival for the patients according to the degree of hepatic dysfunction. For patients with chronic hepatitis and Child-Pugh class A-C cirrhosis, the 5-year survival rates were 35.1%, 10.3%, and 0%, respectively.

Fifteen of the 162 patients in the present series had two courses or more of proton beam therapy; 13 of these had such treatment for tumors judged as newly developed and 2 for tumors judged as locally recurring.

Discussion

In the present series, the 5-year survival rate for 50 patients with a solitary tumor and with least impaired hepatic function (Child-Pugh class A) was 53.5%. It was 57.9% for 15,453 patients with a solitary HCC who underwent surgery from 1988 to 1999 in Japan (8). It is impossible to simply compare these results because the studied patient populations differ entirely. In fact, we have shown that survival of patients with HCC depends largely on the degree of impairment in hepatic function because of coexisting liver cirrhosis and the number of tumors in the liver. However, it can be inferred that proton beam therapy is as effective as hepatectomy for patients with HCC.

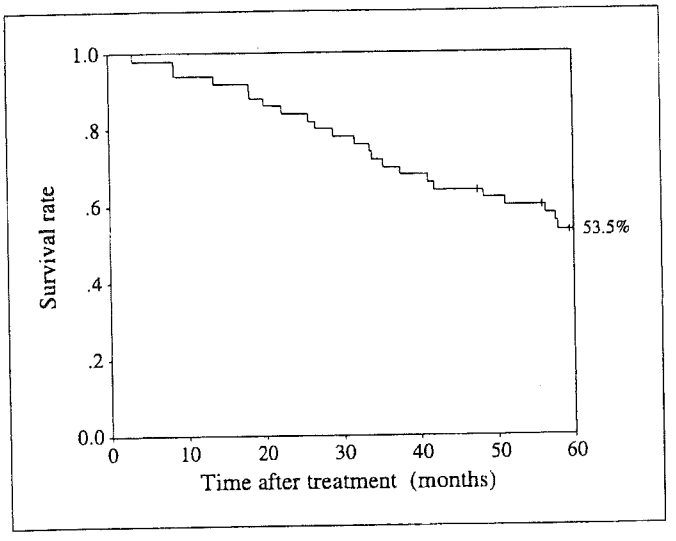

Fig. 4. Survival for patients with least impaired hepatic function (chronic hepatitis or Child-Pugh class A cirrhosis) and a solitary tumor.

Only ~30% of patients with HCC undergo surgery (44). Reasons why patients choose not to undergo surgery include poor medical condition caused by intercurrent diseases to undergo surgery, poor hepatic functions attributable to coexisting liver cirrhosis, advanced age, and too advanced tumor stage. In the present series, 65% of all patients were ages ≥60 years. About half of the patients had multiple tumors and 45% of the patients were class B or C in Child-Pugh classification. Therefore, it seems that the patients with a wider spectrum of general conditions and tumor conditions are treatable with proton beam therapy.

Of patients who underwent percutaneous ethanol injection, microwave coagulation therapy, and radiofrequency ablation from January 1998 to December 1999 in Japan, only a small proportion of the patients had tumors >5 cm (3.5% for percutaneous ethanol injection, 1.8% for microwave coagulation therapy, and 6.4% for radiofrequency ablation; ref. 8). In the present series, 33 of 192 (17.2%) tumors were >5 cm in maximal diameter. The tumor size did not significantly affect local control in the present series, suggesting that proton beam therapy could be used to treat patients with relatively large tumors. We are often unable to detect HCC with ultrasound when it is located at a site adjacent to the lung and the bone. In such cases, we could not treat it with ablative procedures. When a tumor is located at a site adjacent to a larger blood vessel, we are also unable to treat it effectively with radiofrequency ablation because of the heat dissipation through the vessel (45). Smaller (≤3 cm in maximal diameter) multiple tumors are often treated with transcatheter arterial embolization and transarterial chemoembolization. However, it is impossible to use transcatheter arterial embolization/transarterial chemoembolization when the tumor is not fully fed with arteries.

Although we had a better local control rate after initiating the use of respiration gating irradiation (11.8% versus 4.0%), we are unable to assess the degree of its contribution to improvement of local control. Our irradiation techniques, including target delineation, improved considerably during the period. Unfortunately, we have no methodology to distinguish their contributions.

For the same reason, we are unable to identify a tumor that locally recurred because of a geographic miss in treatment planning. Of the 13 tumors that locally recurred in the present

Table 5. Treatment sequelae in 185 courses

Treatment sequelae	No. treatment courses (%)
Acute-subacute	
Elevation of bilirubin	3 (2.1)
Anemia	2 (1.1)
Leukocytopenia	1 (0.5)
Thrombocytopenia	6 (3.2)
Elevation of transaminase level	18 (9.7)
Late	
Infection biloma	2 (1.1)
Common bile duct stenosis	1 (0.5)
Gastrointestinal tract bleeding	2 (1.1)

series, 10 recurred in the central portion of the irradiated volume, whereas the remaining 3 tumors did so at the periphery; some of the 3 tumors that recurred peripherally might have recurred due to a geographic miss.

Of 145 patients who had died as of June 2003, 68 (46.9%) died of tumor progression. On the other hand, the local control rate for all tumor was high (86.9%). The high local control rate with the higher tumor progression rate is explained by the multifocal nature of HCC in the cirrhotic liver; 84% of all patients in the present series developed HCC(s) at a site that was remote from the treated tumor in the liver within 5 years. A significant proportion of them eventually became uncontrollable, engendering patient death. The remaining 77 (53.1%) patients died of various causes unrelated to tumor progression, of whom 55 (37.9% of 145 patient deaths) died of hepatic failure attributable to liver cirrhosis.

No significant difference in local control rate was found between patients with no prior therapy and those previously treated with other modes of therapy, suggesting that a patient with HCC could be treated exclusively with proton beam therapy.

Photon radiotherapy to give 44 to 52 Gy in 4 to 5.5 weeks for patients with HCC yielded a limited improvement in survival and local control rates (46, 47). Robertson et al. (48) and Blomgren et al. (49) recently attempted to increase the dose of irradiation to the hepatic tumors using conformal radiotherapy or stereotactic radiotherapy. Long-term results of their attempts are yet to be shown. In addition, it is unavoidable to have a large portion of the liver and other adjacent organs irradiated with lower doses of deeply penetrating photons. Such treatment may or may not engender late radiation sequelae, including radiation-induced carcinogenesis.

In the present series, most patients were given very high doses compared with those given with photon beams (Table 3), which may explain the higher local control rate obtained in the present series.

Few effective treatments are available for patients having HCC with vascular invasion (50). However, in the present series, 10 patients with a tumor involving major branches of portal veins survived a median 26.4 months after proton beam therapy. Proton beam therapy is the currently preferred treatment for patients having HCC with vascular invasion.

Patients who underwent proton beam therapy had stable performance status before and after irradiation, very few acute reactions to the treatments during and after irradiation, and a few late sequelae after treatment. For those reasons, proton beam therapy seems to be less invasive than any other HCC treatment modalities.

Of the 53 patients who underwent biopsy 3 weeks after completion of irradiation, 14 (26.4%) patients had viable cancer cells. Considering the high rate of local control obtained, second biopsies were undertaken too early after completion of irradiation in the present study.

Fifteen patients had multiple (maximum of four) courses of proton beam therapy, which suggests that proton beam therapy could be given repeatedly at different times. Because HCC in the cirrhotic liver has multifocal carcinogenesis in nature, it renders a great advantage to proton beam therapy in treating patients who often undergo multiple courses of treatments.

Although we could treat most patients with HCC using proton beam therapy, we might not treat a patient who has one or more of the following conditions: poor general condition (performance status 3-4), diffusely infiltrating HCC, multiple HCC (several or more) in both lobes, or an exophytic tumor extensively involving the gastrointestinal tract.

We have started a phase II study in which a proton dose of 60 Gy in 10 fractions over 2 weeks is given to patients having a solitary HCC located not adjacent to the porta hepatis or the gastrointestinal tract. For tumors located adjacent to the porta hepatis and the gastrointestinal tract, we are currently giving 66 Gy in 22 fractions over 4.5 weeks in the hope of avoiding serious late sequelae.

In conclusion, proton beam therapy for patients with HCC is effective, safe, well tolerable, and repeatable. The treatment can apply for cure as well as for palliation to patients with HCC irrespective of tumor size, tumor location in the liver, insufficient feeding of the tumor with arteries, presence of vascular invasion, degree of hepatic dysfunction, and intercurrent diseases.

Acknowledgments

We thank the late Profs. Toshiaki Osuga, Toshio Kitagawa, and Yuji Itai for their dedication to establishing proton beam therapy at Tsukuba.

References

1. Munoz N, Bosch X. Epidemiology of hepatocellular carcinoma, in Okuda K, Ishak KG, editors. Neoplasms of the liver. Tokyo: Springer-Verlag; 1987. p. 3–19.
2. Okuda K, Ohtsuki T, Obata H, et al. Natural history of hepatocellular carcinoma and prognosis in relation to treatment: study of 850 patients. Cancer 1985;56: 918–28.
3. El-Domeiri AA, Huvos AG, Goldsmith HS, et al. Primary malignant tumors of the liver. Cancer 1971;27: 7–11.
4. Nagasue N, Yukaya H, Hamada T, et al. The natural history of hepatocellular carcinoma: a study of 100 untreated cases. Cancer 1984;54:1461–5.
5. The Research Group for Population-Based Cancer Registration in Japan. Cancer incidence and incidence rates in Japan in 1995. Estimates based on data from nine population-based cancer registries. Jpn J Clin Oncol 2000;30:318–21.
6. Nishioka K, Watanabe J, Furuta S, et al. A high prevalence of antibody to the hepatitis C virus in patients with hepatocellular carcinoma in Japan. Cancer 1991;67:429–33.
7. Tanaka K, Hirohata T, Koga S, et al. Hepatitis C and hepatitis B in the etiology of hepatocellular carcinoma in the Japanese population. Cancer Res 1991;51: 2842–7.
8. Ikai I, Itai Y, Okita K, et al. Report of the 15th follow-up survey of primary liver cancer. Hepatol Res 2004;28: 21–9.
9. Nakamura H, Hashimoto T, Oi H, et al. Transcatheter oily chemoembolization of hepatocellular carcinoma. Radiology 1989;170:783–6.
10. Yamada R, Kishi K, Sonomura T, et al. Transcatheter arterial embolization in unresectable hepatocellular carcinoma. Cardiovasc Intervent Radiol 1990;13: 135–9.
11. Bismuth H, Morino M, Sherlock D, et al. Primary treatment of hepatocellular carcinoma by arterial chemoembolization. Am J Surg 1992;163:387–94.
12. Aoyama K, Tsukishiro T, Okada K, et al. Evaluation of transcatheter arterial embolization with epirubicin-lipiodol emulsion for hepatocellular carcinoma. Cancer Chemother Pharmacol 1992;31 Suppl:S55–9.
13. Nakamura H, Mitani T, Murakami T, et al. Five-year survival after transcatheter chemoembolization for hepatocellular carcinoma. Cancer Chemother Phamacol 1994;33 Suppl:S89–92.
14. Tobe T, Arii S. Improving survival after resection of hepatocellular carcinoma: characteristics and current status of surgical treatment of primary liver cancer in Japan. In: Tobe T, Kameda H, et al., editors. Primary liver cancer in Japan. Tokyo: Springer-Verlag; 1992. p. 215–20.
15. Sheu JC, Huang GT, Chen DS, et al. Small hepatocellular carcinoma: intratumor ethanol treatment using new needle and guidance system. Radiology 1987; 163:43–8.
16. Shiina S, Yasuda H, Muto H, et al. Percutaneous ethanol injection in the treatment of liver neoplasms. AJR Am J Roentgenol 1987;149:949–52.
17. Seki T, Wakabayashi M, Nakagawa T, et al. Ultrasonically guided percutaneous microwave coagulation

therapy for small hepatocellular carcinoma. Cancer 1994;74:817–25.
18. Sato M, Watanabe Y, Ueda S, et al. Microwave coagulation therapy for hepatocellular carcinoma. Gastroenterology 1996;110:1507–14.
19. Rossi S, Fornari F, Buscarini L. Percutaneous ultrasound-guided radiofrequency electrocautery for the treatment of small hepatocellular carcinoma. J Intervent Radiol 1993;8:97–103.
20. Rossi S, Buscarini L, Garbagnati F, et al. Percutaneous treatment of small hepatic tumors by an expandable RF needle electrode. AJR Am J Roentgenol 1998;170:1015–22.
21. Buscarini L, Buscarini E, Di Stasi M, et al. Percutaneous radiofrequency ablation of small hepatocellular carcinoma: long-term results. Eur Radiol 2001;11:914–21.
22. Phillips R, Murikami K. Primary neoplasms of the liver. Results of radiation therapy. Cancer 1960;13:14–20.
23. Cochrane AMG, Murray-Lyon IM, Brinkley DM, et al. Quadruple chemotherapy versus radiotherapy in treatment of primary hepatocellular carcinoma. Cancer 1977;40:609–14.
24. Friedman MA, Volberding PA, Cassidy MJ, et al. Therapy of hepatocellular carcinoma with combined intrahepatic arterial chemotherapy and whole liver irradiation. Ann Acad Med Singapore 1980;9:260–3.
25. Russell AH, Clyde C, Wasserman TH, et al. Accelerated hyperfractionated hepatic irradiation in the management of patients with liver metastases: result of the RTOG dose escalating protocol. Int J Radiat Oncol Biol Phys 1993;27:117–23.
26. Osuga T, Matsuzaki Y, Chiba T, et al. Radiatiotherapy. In: Okuda K, Tabor E, editors. Liver cancer. London: Churchill Livingstone; 1997. p. 481–96.
27. Suit H, Urie M. Proton beams in radiation therapy. J Natl Cancer Inst 1992;84:155–64.
28. Tsujii H, Tsuji H, Inada T, et al. Clinical results of fractionated proton therapy. Int J Radiat Oncol Biol Phys 1992;25:49–60.
29. Tanaka N, Matsuzaki Y, Chuganji Y, et al. Proton irradiation for hepatocellular carcinoma. Lancet 1992;340:1358.
30. Matsuzaki Y, Osuga T, Saito Y, et al. A new, effective, and safe therapeutic option using proton irradiation for hepatocellular carcinoma. Gastroenterology 1994;106:1032–41.
31. Tsujii H, Tsuji H, Okumura T, et al. Proton therapy of thoraco-abdominal tumors. In: Linz U, editor. Ion beams in tumor therapy. London: Chapman & Hall; 1995. p. 127–32.
32. Edmondson HA, Steiner PE. Primary carcinoma of the liver: a study of 100 cases among 48,900 necropsies. Cancer 1954;7:462–503.
33. Pugh RNH, Murray-Lyon IM, Dawson JL, et al. Transection of the oesophagus for bleeding oesophageal varices. Br J Surg 1973;60:646–9.
34. International Union Against Cancer (UICC). TNM classification of malignant tumours. 6th ed. New York: Wiley-Liss; 2002. p. 81–3.
35. Inada T, Hayakawa Y, Maruhashi A, et al. Vertical proton beam irradiation control system for cancer therapy. Nippon Acta Radiol 1984;44:844–53.
36. Inada T, Tsuji H, Hayakawa Y, et al. Proton irradiation synchronized with respiratory cycle. Nippon Acta Radiol 1992;52:1161–7.
37. Ohara K, Okumura T, Akisada M, et al. Irradiation synchronized with respiration gate. Int J Radiat Oncol Biol Phys 1989;17:853–7.
38. Fowler JF. The linear-quadratic formula and progress in fractionated radiotherapy. Br J Radiol 1989;62:679–94.
39. WHO handbook for reporting results of cancer treatment. WHO offset publication No. 48. Geneva: WHO; 1979.
40. Cox JD, Stetz J, Pajak TF. Toxicity criteria of the Radiation Therapy Oncology Group (RTOG) and the European Organization for Research and Treatment of Cancer (EORTC). Int J Radiat Oncol Biol Phys 1995;31:1341–6.
41. Kaplan EL, Meier P. Nonparametric estimation from incomplete observations. J Am Stat Assoc 1958;53:457–81.
42. Peto R, Pike MC, Armitage P, et al. Design and analysis of randomized clinical trials requiring prolonged observation of each patient. II. Analysis and examples. Br J Cancer 1977;35:1–39.
43. Cox DR. Regression models and life tables. J Roy Stat Soc Sec 1972;B34:187–220.
44. Hassoun Z, Gores GJ. Treatment of hepatocellular carcinoma. Clin Gastroenterol Hepatol 2003;1:10–8.
45. Yamasaki T, Kurokawa F, Shirahashi H, et al. Percutaneous radiofrequency ablation therapy for patients with hepatocellular carcinoma during occlusion of hepatic blood flow. Cancer 2002;95:2353–60.
46. Cheng JCH, Chuang VP, Cheng SH, et al. Local radiotherapy with or without transcatheter arterial chemoembolization for patients with unresectable hepatocellular carcinoma. Int J Radiat Oncol Biol Phys 2000;47:435–42.
47. Yasuda S, Ito H, Yoshikawa M, et al. Radiotherapy for large hepatocellular carcinoma combined with transcatheter arterial embolization and percutaneous ethanol injection therapy. Int J Oncol 1999;15:467–73.
48. Robertson JM, Lawrence TS, Dworzanin LM, et al. Treatment of primary hepatobiliary cancers with conformal radiation therapy and regional chemotherapy. J Clin Oncol 1993;11:1286–93.
49. Blomgren H, Lax I, Göranson H, et al. Radiosurgery for tumors in the body: clinical experience using a new method. J Radiosurg 1998;1:63–74.
50. Yamada K, Izaki K, Sugimoto K, et al. Prospective trial of combined transcatheter arterial chemoembolization and three-dimensional conformal radiotherapy for portal vein tumor thrombus in patients with unresectable hepatocellular carcinoma. Int J Radiat Oncol Biol Phys 2003;57:113–9.

Available online at www.sciencedirect.com
SCIENCE DIRECT
Biochimica et Biophysica Acta 1745 (2005) 401 – 410
BIOCHIMICA ET BIOPHYSICA ACTA
BBA
http://www.elsevier.com/locate/bba

Rapid inhibition of MAPK signaling and anti-proliferation effect via JAK/STAT signaling by interferon-α in hepatocellular carcinoma cell lines

Kentaro Inamura[a,b], Yasushi Matsuzaki[b], Naoya Uematsu[a], Akira Honda[b], Naomi Tanaka[b], Kazuhiko Uchida[a,*]

[a]*Department of Molecular Biology and Molecular Oncology, Graduate School of Comprehensive Human Science, University of Tsukuba, 1-1-1 Tennoudai, Tsukuba, Ibaraki 305-8575, Japan*
[b]*Department of Gastroenterology, Institute of Clinical Medicine, University of Tsukuba, 1-1-1 Tennodai, Ibaraki 305-8575, Tsukuba, Japan*

Received 19 April 2005; received in revised form 9 June 2005; accepted 10 June 2005
Available online 29 June 2005

Abstract

The potential anti-proliferation effect of interferon-alpha (IFN-α) against hepatocellular carcinoma (HCC) and its growth inhibitory mechanisms remain unclear. We examined four human HCC cell lines and every cell line had the anti-proliferative effect of IFN-α. The PLC/PRF/5 cell line, which expressed the IFN receptor most abundantly, responded most effectively to IFN-α stimulation. Here, we delineate the anti-proliferative effect of IFN-α via the MAPK pathway in human HCC cell lines. IFN-α retarded G1/S transition with no evidence of apoptosis and inhibited cell proliferation. IFN-α diminished the phosphorylation of both extracellular signal-regulated kinase (ERK) and mitogen-activated ERK-regulating kinase (MEK), but not Raf, within 5 min. Knockdown of signal transducers of activation and transcription1 (STAT1) or Janus kinase1 (JAK1) suppressed the reduction of phosphorylation both of ERK and MEK and diminished the growth inhibition by IFN-α. These results suggest that IFN-α induces anti-proliferative signaling via the JAK/STAT pathway downstream of IFN-α receptors and may reduce the growth stimulation signaling by cross-talk with the MEK/ERK pathway without IFN-α-induced transcription.

Keywords: Interferon (IFN); Extracellular signal-regulated kinase (ERK); Mitogen-activated ERK-regulating kinase (MEK); Signal transducers of activation and transcription1 (STAT1); Janus kinase1 (JAK1); Small interfering RNA (siRNA)

1. Introduction

Hepatocellular carcinoma (HCC) is the fifth most common malignant disorder and causes about 1 million deaths a year worldwide. Hepatocellular carcinoma is more common in Asia and Africa than in other continents. About 80% of patients with HCC also have liver cirrhosis. Chronic infection with hepatitis B virus and hepatitis C virus increases the risk of developing HCC. HCC is a malignant tumor of hepatocellular origin that develops in patients with risk factors that include alcohol abuse, viral hepatitis, and metabolic liver disease; aflatoxins have also been implicated as a risk factor for HCC. In spite of aggressive treatments for HCC including hepatectomy, transarterial embolization with percutaneous ethanol injection therapy, and radio-frequency ablation, most patients show disease recurrence that finally progresses to the advanced stages with vascular invasion and multiple intrahepatic metastases. Thus, prognosis for HCC is generally poor and the 5-year survival rate is limited to 25–58% after surgery [1].

IFNs are crucial and potent components of the early response against virus infection and are used for the medical treatment of hepatitis C and hepatitis B as well as solid tumors and hematologic malignancies [2,3]. IFN therapy improves the survival rate of patients with chronic hepatitis C by preventing liver-related causes of death including liver dysfunction and HCC. Studies have compared IFN-treated patients to untreated patients regarding overall mortality and observed higher mortality in untreated patients [4]. IFN also

* Corresponding author. Fax: +81 29 855 5271.
E-mail address: kazuhiko.uchida@cbiri.org (K. Uchida).

0167-4889/$ - see front matter © 2005 Elsevier B.V. All rights reserved.
doi:10.1016/j.bbamcr.2005.06.003

prevents recurrence of HCC after complete resection or ethanol injection treatment, even if hepatitis C virus cannot be eradicated. The group not treated with IFN showed 70% recurrence while the treated group showed 10% [5]. In nude mice, IFN inhibits metastasis and angiogenesis of HCC after curative resection [6]. Thus, IFN is expected to function in the chemoprevention of HCC.

Recently, interferon-alpha (IFN-α) has been used as a chemotherapeutic agent in combination with anti-cancer drugs against HCC. Generally, IFN-α is administered along with several chemotherapeutic agents such as 5-FU/IFN-α or 5-FU/IFN-α/cisplatin/methotrexate and doxorubicin to patients with advanced and unresectable HCC [7–9]. These clinical trails have demonstrated the considerable effectiveness of IFN in patients with HCC; yet how IFN-α modulates the anti-tumor activity of anticancer drugs like 5-FU against HCC cells remains unclear. IFN therapy improves the survival rate of patients with chronic hepatitis C by preventing liver-related causes of death [4] and inhibits intrahepatic recurrence in HCC with chronic hepatitis C [10]. Because of the complex genetic background of HCC, any given therapeutic approach may yield inconsistent results and different responses. Without the identification of an adequate molecular target, interpreting and validating the results of clinical trials are difficult.

IFN-α has been initially described as an antiviral cytokine that affects the growth and differential function of various cell types [11]. IFN acts with transducing regulatory signals through the Janus tyrosine kinase/signal transducers of activation and transcription (JAK/STAT) pathway [12]. IFN-α receptor engagement initiates signals that are transmitted from the cell surface to the nucleus. Upon ligand binding to the IFN-α receptor, the receptor-associated Janus family kinases, Tyk2 and JAK1, are auto-phosphorylated on tyrosine residues and the tyrosine phosphorylation activates the cytoplasmic latent signal transducer and activators of transcription factors STAT1 and STAT2. STAT1 has two isoforms: STAT1-α (91 kDa) and STAT1-β (84 kDa). STAT1-β is a naturally occurring splice variant of STAT1-α that lacks 38 carboxy-terminal amino acids [13]. Activated STAT1/STAT1 homodimers and STAT1/STAT2 heterodimers translocate to the nucleus, where they bind with p48 to form the interferon-stimulated gene factor-3 (ISGF-3) trimeric complex. The ISGF-3 complex recognizes and binds to the interferon-stimulated response element (ISRE) sequence in the regulatory regions of the genes. Certain IFN-α-inducible proteins, such as double-stranded RNA-activated protein kinase (PKR) [14], 2′,5′-oligoadenylate synthetase (OAS), and Mx proteins mediate the antiviral actions. However, the signal transduction pathway for the anti-proliferative effect of IFN-α is not fully understood. The p53 gene is transcriptionally induced by IFN-α/β through ISGF-3 activation accompanied by an increase in p53 protein level, but IFN-α/β signaling itself does not activate p53; rather, it contributes to boosting the p53 responses to stress signals, such as 5-FU, X-ray irradiation, and viral infection [15].

The signaling pathways employing extracellular-regulated kinase (ERK) and mitogen-activated ERK-activating kinase (MEK) are critical in growth factor signaling. These pathways are fundamental in controlling cell development and activation proliferation [16].

In the CD4+ lymphoblastoid and monocytoid cell lines [17] and in CD4+ T cells [18], IFN-α inhibits activation of the MEK/ERK pathway. However, CD4+ lymphoblastoid and monocytoid cells need 24–48 h to affect MEK and ERK1/2 signaling after IFN-α treatment; no effect was observed upon short-term exposure until 30 min. Suppression of cell proliferation of CD4+ T cells needs at least 2 h to activate cell growth inhibition signals.

In this study, we intend to delineate the rapid response of the anti-proliferative action of IFN-α via the MAPK pathway in human HCC cell lines. Using small interfering RNA (siRNA) technology, we investigated the enhancement of phosphorylation of MEK and ERK and blocked the inhibition of phosphorylation of MEK and ERK by IFN-α. Our results suggest the cross-talk of the JAK/STAT pathway activated by IFN-α and the MAPK pathway with rapid inhibition of MAPK signaling not due to de novo protein synthesis and/or transcriptional activation of downstream genes.

2. Materials and methods

2.1. Cell cultures and cytokines

Human HCC cells lines HepG2, Hep3B, PLC/PRF/5, and HuH7 (all from Cell Resource Center for Biomedical Research Institute of Development, Aging and Cancer, Tohoku University) were grown in Dulbecco's modified Eagle's medium (Nissui, Tokyo, Japan) supplemented with 10% fetal calf serum (FCS). Cells were treated with recombinant human IFN-α (IFN-α2a; Roche) after incubation in serum-free medium for 48 h, and either left unstimulated or stimulated with IFN-α (0, 50, 100, 500, and 1000 units/ml) with 10% FCS medium. When cells were assayed until 8 days, IFN-α was added every 48 h at a concentration as indicated.

2.2. Cell proliferation analysis and IFN-α treatment

To analyze the effect of IFN-α on cell proliferation, cells were grown without FCS for 48 h, and then received fresh medium including 10% FCS with or without IFN-α. Interferon-α was added to the medium at a concentration of 0, 50, 100, 500, or 1000 units/ml. A proliferation assay was performed by analyzing the number of viable cells from the cleavage of tetrazolium salts added to the culture medium with WST-1 (Roche) according to the manufacturer's protocol. Briefly, HCC cells (HepG2, Hep3B, PLC/

PRF/5, and HuH7) at a concentration of 5×10^3 cells/200 μl medium/well were seeded in 96-well plates. After the incubation period (Days 0, 2, 4, 6, and 8), WST-1 was added at 10 μl/well and the cells were incubated for 4 h. Absorbance of the samples against a background control as a blank was measured using a microtiter plate reader (Tecan, Männedorf, Switzerland). This experiment was repeated four times.

2.3. DNA synthesis assay

DNA synthesis and its inhibition by IFN-α were measured by 5-bromo-2′-deoxy-uridine (BrdU) incorporation into DNA. Cells from each cell line were seeded in quadruplicate in a 96-well plate in a volume of 5×10^3 cells/200 μl medium/well and cultivated in medium containing 10% FCS. After incubation for 24 h, DNA synthesis was assayed with a commercial cell proliferation enzyme-linked immunosorbent assay (ELISA) kit (Roche) according to the manufacturer's instructions.

2.4. Flow cytometry

The cells (2×10^6) were harvested from culture dishes with trypsinization, washed in phosphate-buffered saline (PBS), suspended in 200 μl of ice-cold 70% ethanol, and incubated on ice for at least 1 h. The cells were washed with PBS, exposed to RNase A (Sigma), and incubated at 37 °C for 30 min. The cells were then suspended in propidium iodide (Sigma) in PBS, and DNA analysis was performed using fluorescence-activated cell sorting (FACS) with a FACSAria™ instrument (Becton Dickinson, San Jose, CA) emitting a 488-nm beam. The cell cycle was evaluated by measuring the percentage of G0/G1-, S-, and G2/M-phase cells, at time points of 0 (control), 8, 16, 24, and 32 h after treatment with IFN-α. Every experiment was repeated four times.

Flow cytometry of annexin V-stained and propidium iodide-stained cells was also performed to detect apoptotic cells. Briefly, 1×10^6 cells were washed and resuspended in HEPES buffer [10 mM HEPES (pH 7.4), 140 mM NaCl, and 5 mM $CaCl_2$] containing annexin V (1:50 v/v) and 1 μg/ml of propidium iodide for 15 min, and then analyzed by flow cytometry.

2.5. Immunoblotting

The activities of Raf, MEK, and ERK signaling cascades were assessed by the immunoblotting of cell lysates and probing with anti-phospho-Raf, anti-phospho-MEK, anti-phospho-ERK1/2, and anti-ERK1/2 antibodies (Cell Signaling Technologies, Beverly, MA). Anti-IFN-α/β receptor antibody was from Santa Cruz Biotechnology (Santa Cruz, CA), anti-protein kinase R (anti-PKR), and anti-phospho-STAT1 antibodies were purchased from Cell Signaling Technologies, and anti-STAT1 antibody was purchased from Sigma (St. Louis, MO). Quantification of all blots was performed by densitometry analysis using the LAS-3000 densitometer and Multi Gauge Version 2.2 software from Fuji Photo Film (Tokyo, Japan).

2.6. Immunoprecipitation of STAT1 and MEK

Cells were washed twice with ice-cold PBS; ice-cold NP-40 buffer [50 mM Tris–HCl (pH 8.0), 150 mM NaCl, and 1% NP-40, supplemented with protease inhibitors cocktail (Sigma)] was added at 1 ml per 10^7 cells/100 mm dish. The cell lysate was centrifuged at $14{,}000\times g$ for 15 min and the supernatant fraction was transferred to a fresh centrifuge tube to which was added 10 μl of protein G agarose bead slurry (50%) per 1 ml of cell lysate. The cell lysate solution was incubated at 4 °C for 10 min on an orbital shaker and the protein G agarose beads were removed by centrifugation. The cell lysate was diluted to 1 mg/ml total cell protein with PBS and 5 μg of anti-MEK or anti-STAT antibodies was added to 1 ml of cell lysate. The cell lysate/antibody mixture was incubated for 2 h at 4 °C; 10 μl protein G agarose bead slurry was added and the mixture was rocked gently for 1 h at 4 °C. The agarose beads were collected by centrifugation and the supernatant was discarded. The beads were washed twice with PBS and resuspended in 60 μl of 2× sample buffer, then boiled for 5 min. The supernatant fraction components were separated by SDS-PAGE.

2.7. siRNA-mediated knockdown of STAT1 and JAK1

The siRNA oligomer targeted to STAT1 (Cell Signaling Technology) and JAK1 (Ambion, Austin, TX) were used for suppression of JAK/STAT signaling. Cells were seeded at 50% confluence 1 day before transfection and transfected using Transfection Reagent (Mirus) according to the manufacturer's protocol. Successful transfection of siRNA was confirmed by fluorescent detection of SignalSilence™ control siRNA (Cell Signaling Technology) and Western blotting analysis of STAT1 and JAK1 confirmed knockdown of STAT1 and JAK1.

2.8. Phosphatase assay

A commercial serine/threonine phosphatase assay system was purchased from Promega (Madison, WI). The activities of protein phosphatase (PP) 2A, PP2B, and PP2C were measured according to the manufacturer's protocol. Briefly, the assay began with a standard phosphatase reaction performed in the reaction buffer with the provided phosphorylated bisamide rhodamine 110 peptide substrate and 7-amino-4-methycoumarin (AMC) control substrate. Following the phosphatase reaction, protease solution was added to simultaneously stop the phosphatase reaction and completely digest the dephosphorylated serine/threonine PPase rhodamine 110 substrate and AMC substrate, producing highly fluorescent rhodamine 110 and AMC.

Phosphorylated serine/threonine PPase rhodamine substrate was resistant to protease digestion and remained non-fluorescent. Thus, the rhodamine 110 fluorescence intensity measured in the assay correlated with phosphatase activity in the presence of protease, and the AMC fluorescence intensity was an indication of protease activity.

2.9. Statistical analysis

Data from each experiment are expressed as mean ± S.E. Differences between groups were examined for statistical significance using Student's *t*-test. All of the experiments were repeated more than four times and reproducible results were obtained.

3. Results

3.1. IFN-α treatment reduces cell proliferation and DNA synthesis in HCC cell lines in a dose-dependent manner

We investigated the effect of IFN-α on the inhibition of cell proliferation in the four HCC cell lines HepG2, Hep3B, PLC/PRF/5, and HuH7 by a cell proliferation assay using WST-1 up to 8 days after IFN-α treatment. After incubation in serum-free medium for 48 h, HCC cells were exposed to IFN-α at the concentrations of 0 (control), 50, 100, 500, and 1000 units/ml with 10% FCS. Among these cell lines, PLC/PRF/5 and HuH7 were the most effective in suppression (Fig. 1A, B). At Day 8 following IFN-α treatment with 1000 units/ml, PLC/PRF/5 showed 31% reduction and HuH7 showed 25% reduction. Following treatment with 500 units/ml of IFN-α, proliferation of PLC/PRF/5 showed 21% reduction. A dose-dependent anti-proliferative effect was assessed in PLC/PRF/5 at more than 50 units/ml of IFN-α and in HuH7 at the concentrations of 500 and 1000 units/ml at Day 8 after IFN-α treatment. Statistical significance in suppression was observed in PLC/PRF/5 at the concentration of 500 units/ml and 1000 units/ml and HuH7 at the concentration of 1000 units/ml of IFN-α ($P<0.01$). The cell line PLC/PRF/5 showed a statistically significant reduction ($P<0.05$) at Day 2 and Day 4 at the concentration of 500 units/ml and 1000 units/ml (Fig. 1A). However, HepG2 and Hep3B did not demonstrate a statistically significant reduction (data not shown).

To determine whether IFN-α dependent suppression of proliferation is due to IFN-α-dependent inhibition of DNA synthesis in HCC cells, we performed a BrdU incorporation assay and flow cytometry. As in the WST-1 assay, after incubation with FCS-free medium for 48 h before IFN treatment, HepG2, Hep3B, PLC/PRF/5, and HuH7 cells were incubated in medium with 10% FCS plus IFN-α at a concentration of 0 (control), 50, 100, 500, or 1000 units/ml. The PLC/PRF/5 cell line was the most influential among the four cell lines and had 29% reduction of DNA synthesis by IFN at 1000 units/ml compared with the control ($P<0.01$) (Fig. 1C). The HuH7 cell line also showed decreased DNA synthesis ($P<0.05$).

3.2. IFN-α prevented cell cycle progression in HCC cells

Several studies have shown that IFN-α reduces cell cycles by arresting the cells in the G0/G1 phase in a variety of cell lines [2,19,20]. Using PLC/PRF/5 cells, which were most sensitive to IFN-α, we performed flow cytometry analysis to determine cell cycle progression at 0, 8, 16, 24, and 32 h after incubation with 1000 units/ml IFN-α. The percentage of cells in G0/G1 was 82% and that in the S phase was 14% after serum-starvation for 48 h (at 0 time after serum plus IFN addition). Cells without IFN-α treatment showed a decrease of 49% in G0/G1 and an increase to 39% in the S phase 16 h after serum addition. On the other hand, IFN-α prevented entry into the S phase from G0/G1; as a result, the G0/G1 population was increased to 59% and the S phase population was decreased to 34% at 16 h, and 26% of cells were still in the S phase at 24 h, when 24% of the S phase cells were observed in untreated HCC cells (Fig. 2). These data suggest that IFN-α treatment retards cell cycle progression after serum stimulation in HCC cells. Annexin V fluorescence was not detected in IFN-α-treated cells, indicating no apoptotic cells in this fraction (data not shown).

3.3. Expression of the IFN receptor

We examined the quantification of IFN-α receptors in four human hepatocellular carcinoma cell lines (HepG2, Hep3B, PLC/PRF/5, and HuH7) with anti-human IFN α/β receptor antibody with a molecular weight of 60 kDa (Fig. 3A). On gel electrophoresis, 20 μg of each whole-cell lysate was applied and equal amounts of total protein were confirmed by α-tubulin. The PLC/PRF/5 cell line expressed the IFN receptor most abundantly, about twice the intensity of other cell lines.

3.4. Signal transduction via IFN receptor in HCC cells

To confirm the IFN-α signals and the subsequent JAK/STAT pathway activation, we checked the expressions of STAT1 and phosphorylated STAT1 at the times of 0, 5, 15, 30, and 60 min after stimulation with 1000 units/ml IFN-α in PLC/PRF/5 cells (Fig. 3B). Upon the binding of IFN-α to the IFN-α/β receptors, Tyk2 and JAK1 are autophosphorylated on the tyrosine residues and their phosphorylated forms activate the cytoplasmic latent signal transducer, including the transcription factors STAT1 and STAT2. STAT1 was expressed at all time points; the phosphorylated STAT1, which was not detected before stimulation, was detected within 5 min after stimulation and increased to its highest intensity at 30 min, then decreased (Fig. 3B).

Activated STAT1/STAT1 homodimers and STAT1/STAT2 heterodimers translocate to the nucleus, where they

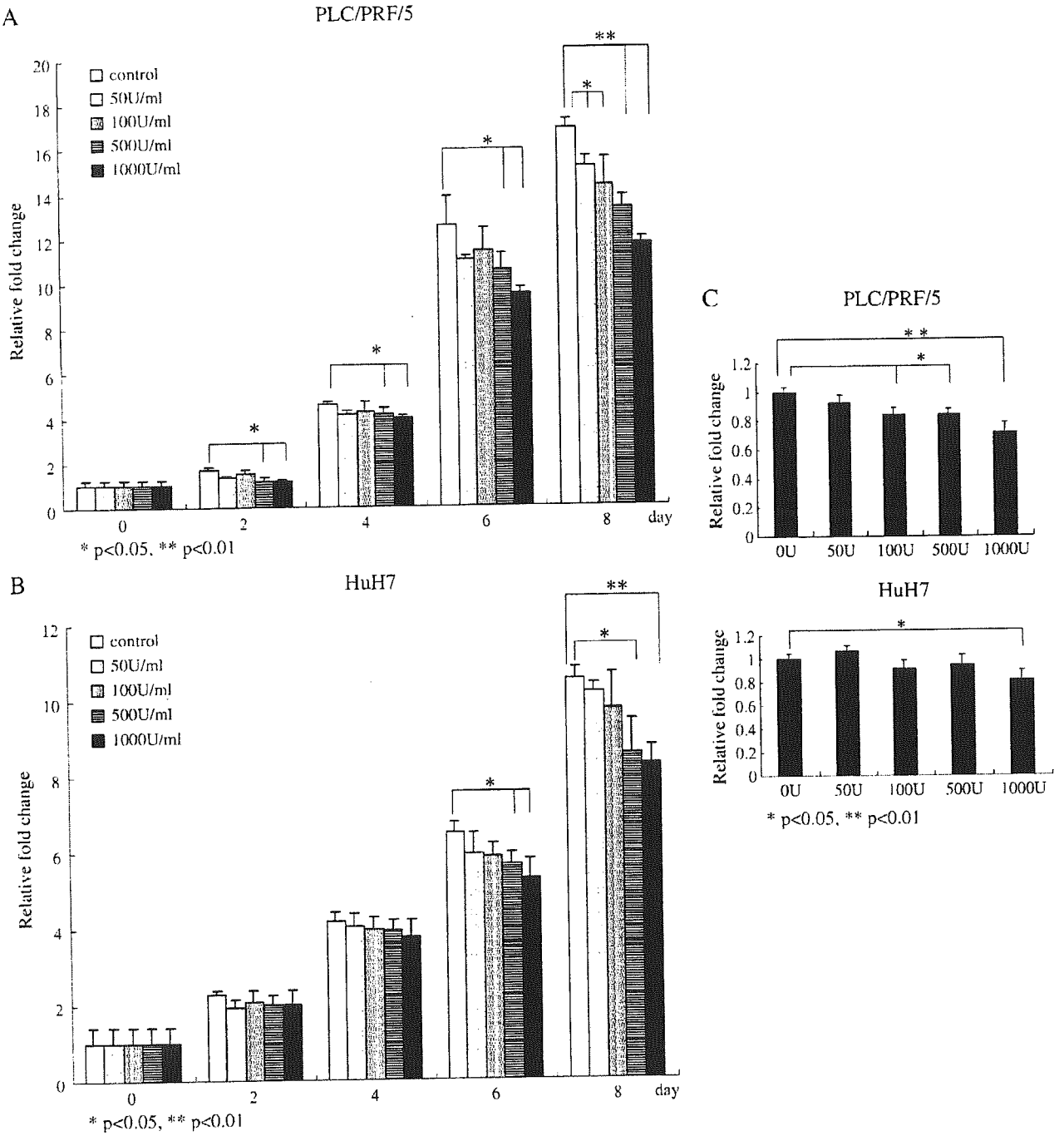

Fig. 1. Growth inhibition of hepatocellular carcinoma by IFN-α. Cell proliferation curves of cell lines HepG2, Hep3B (data not shown), (A) PLC/PRF/5, and (B) HuH7 are indicated up to 8 days, assayed by WST-1 with or without the addition of 50, 100, 500, and 1000 units/ml of IFN-α. Data are shown as means of four trials for each experiment. IFN-α significantly reduced cell growth of PLC/PRF/5 to 21% at 500 units/ml and 31% at 1000 units/ml relative to the control ($P<0.01$). The HuH7 cell line showed a 25% reduction in cell growth at 1000 units/ml ($P<0.01$). (C) DNA synthesis assayed by BrdU incorporation. The PLC/PRF/5 cell line showed the most efficient inhibition among the four cell lines. Interferon-α induced a 29% reduction of DNA synthesis at 1000 units/ml compared with the 0 time control. HepG2 and Hep3B had reductions but they were not statistically significant (data not shown). Data are shown as the means of four trials for each experiment and each error bar shows the standard deviation.

bind with p48 to form the interferon-stimulated gene factor-3 (ISGF-3) trimeric complex; ISGF-3 recognizes and binds to the interferon-stimulated response element (ISRE) sequence in the regulatory regions of the genes and creates several antiviral proteins including PKR [21]. We checked PKR expression as evidence of the IFN response. At 0, 1, 6, 12, and 24 h after incubation with 1000 units/ml of IFN-α, the expression of PKR protein in PLC/PRF/5 cells was

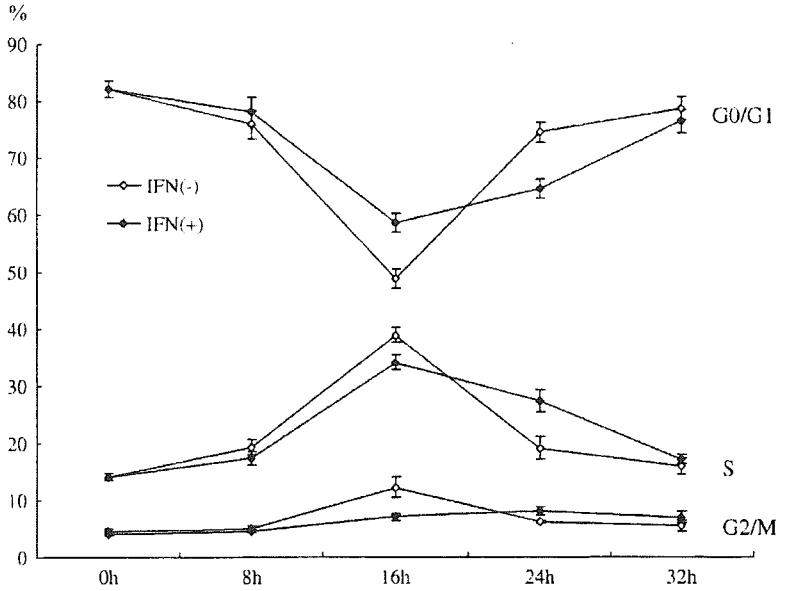

Fig. 2. Cell cycle retardation in IFN-α-treated PLC/PRF/5 cells. At 16 h, the G0/G1 cell population decreased to 49% and the S phase cell population increased to 39% in medium without IFN-α; however, in IFN-α-treated cells, the G0/G1 population decreased to 59% and the S phase population decreased to 34%. In PLC/PRF/5 cells, IFN-α prolonged the transition from G0/G1 and the entry into the S phase.

analyzed (Fig. 3C). The expression of PKR increased gradually 24 h after IFN-α treatment. These results indicate that, in PLC/PRF/5 cells, JAK/STAT signaling via IFN receptors induces transcriptional activation of a downstream gene in response to IFN-α. The JAK/STAT signaling had a peak at 30 min and induction of PKR expression took more than 6 h.

3.5. IFN-α inhibits activation of the MEK/ERK pathway before JAK/STAT activation but does not inhibit Raf-1 activity

The MEK/ERK pathway is pivotal for cell proliferation and activation and MEK activation requires the upstream kinases Raf-1 and Ras [22,23]. We examined whether IFN-α signaling affected the phosphorylation of Raf-1, MEK, and ERK1/2 in the suppression of the proliferation of HCC cells. The PLC/PRF/5 cells were incubated with serum-starved medium for 48 h; then, fresh serum with or without 1000 units/ml IFN-α was added. After incubation for 0, 5, 15, 30, and 60 min, the levels of phosphorylation of Raf, MEK, and ERK1/2 were assessed to compare IFN-α-treated cells to control cells. Levels of phospho-Raf-1, phospho-MEK, phospho-ERK1/2, MEK, and ERK1/2 at the time of 5 min are shown in Fig. 4A. As a result, IFN-α reduced the phosphorylation of MEK (47% reduction) and the phosphorylation of ERK1/2 (41% reduction) 5 min after treatment ($P<0.05$) (Fig. 4B). Phosphorylation of ERK1/2 showed statistically reduction at 30 min and 60 min after treatment (data not shown), but phosphorylation of MEK was not significantly reduced. However, phosphorylation of Raf-1 did not show any difference between cells treated with and without IFN-α. These results suggest that IFN-α sets in motion a cascade of events within the first 5 min of treatment, leading to the reduction of MEK and ERK1/2 functions. Although we tested whether IFN-α treatment induced a protein interaction between STAT and MEK by immunoprecipitation using both STAT and MEK antibodies, we detected neither STAT in the MEK precipitate nor MEK in the STAT precipitate (data not shown).

3.6. Knockdown of STAT1 and JAK1 diminished the effect of IFN-α and enhanced the phosphorylation of MEK and ERK

We achieved successes knockdown of STAT1 and JAK1 with siRNA treatment (Fig. 5A). Phosphorylation of MEK and ERK1/2 was reduced and suppression of STAT1 and JAK1 by siRNA results in abolishment IFN effect on MEK/ERK phosphorylation by IFN-α treatment (Fig. 5B, C). Phosphorylation of MEK and ERK1/2 was relatively enhanced by knockdown of STAT1 and JAK1 with siRNA treatment. Moreover, knockdown of STAT1 and JAK1 with siRNA treatment attenuated the anti-proliferative effect of IFN-α treatment (Fig. 5D) assayed by WST-1.

4. Discussion

The present study revealed that IFN-α induced rapid down-regulation of MEK and ERK1/2 phosphorylation in